

AD-A100 276

TECHNICAL
LIBRARY

AD

CONTRACT REPORT ARBRL-CR-00451

DEVELOPMENT OF A TWO-DIMENSIONAL
IMPLICIT INTERIOR BALLISTICS CODE

Prepared by

Scientific Research Associates, Inc.
P. O. Box 498
Glastonbury, CT 06033

March 1981



US ARMY ARMAMENT RESEARCH AND DEVELOPMENT COMMAND
BALLISTIC RESEARCH LABORATORY
ABERDEEN PROVING GROUND, MARYLAND

Approved for public release; distribution unlimited.

DTIC QUALITY INSPECTED

Destroy this report when it is no longer needed.
Do not return it to the originator.

Secondary distribution of this report by originating
or sponsoring activity is prohibited.

Additional copies of this report may be obtained
from the National Technical Information Service,
U.S. Department of Commerce, Springfield, Virginia
22161.

The findings in this report are not to be construed as
an official Department of the Army position, unless
so designated by other authorized documents.

*The use of trade names or manufacturers' names in this report
does not constitute endorsement of any commercial product.*

UNCLASSIFIED

SECURITY CLASSIFICATION OF THIS PAGE (When Data Entered)

REPORT DOCUMENTATION PAGE		READ INSTRUCTIONS BEFORE COMPLETING FORM
1. REPORT NUMBER CONTRACT REPORT ARBRL-CR-00451	2. GOVT ACCESSION NO.	3. RECIPIENT'S CATALOG NUMBER
4. TITLE (and Subtitle) Development of a Two-Dimensional Implicit Interior Ballistics Code		5. TYPE OF REPORT & PERIOD COVERED Draft Final report Aug. 20, 1979-Nov. 20, 1980
		6. PERFORMING ORG. REPORT NUMBER
7. AUTHOR(e) Howard J. Gibeling Henry McDonald		8. CONTRACT OR GRANT NUMBER(e) DAAK11-79-C-0098
9. PERFORMING ORGANIZATION NAME AND ADDRESS Scientific Research Associates, Inc. P.O. Box 498 Glastonbury, CT 06033		10. PROGRAM ELEMENT, PROJECT, TASK AREA & WORK UNIT NUMBERS
11. CONTROLLING OFFICE NAME AND ADDRESS US Army Armament Research and Development Command US Army Ballistic Research Laboratory ATTN: DRDAR-BL Aberdeen Proving Ground, MD 21005		12. REPORT DATE March 1981
		13. NUMBER OF PAGES 60
14. MONITORING AGENCY NAME & ADDRESS (if different from Controlling Office)		15. SECURITY CLASS. (of this report) UNCLASSIFIED
		15a. DECLASSIFICATION/DOWNGRADING SCHEDULE
16. DISTRIBUTION STATEMENT (of this Report) Approved for public release; distribution unlimited.		
17. DISTRIBUTION STATEMENT (of the abstract entered in Block 20, if different from Report)		
18. SUPPLEMENTARY NOTES		
19. KEY WORDS (Continue on reverse side if necessary and identify by block number) Multidimensional Implicit Numerical Method Two-phase Reacting Flow Gun Interior Ballistics Transient Combustion Time-dependent Adaptive Grid		
20. ABSTRACT (Continue on reverse side if necessary and identify by block number) The governing partial differential equations and constitutive relations are presented for the two-phase, axisymmetric, turbulent flow in a gun tube with a rotating projectile. The formulation includes the following constitutive models: Noble-Abel gas equation of state, molecular viscosity and thermal conductivity, turbulent viscosity and length scale, intergranular stress relation, interphase drag and heat transfer relations, and a burning rate correlation for solid phase combustion. One-dimensional heat conduction models are utilized to obtain both the barrel wall surface temperature and (CONTINUED)		

UNCLASSIFIED

SECURITY CLASSIFICATION OF THIS PAGE(*When Data Entered*)

20. ABSTRACT (Continued).

the average solid particle surface temperature. An axisymmetric time-dependent adaptive coordinate system for interior ballistics flow field calculations is presented, and distinct filler elements and the projectile are treated using a quasi-one-dimensional lumped parameter analysis.

The existing computer code ALPHA has been modified to include both an ignition model and capability to treat geometries in which the tube radius is a function of axial distance. The governing equations in the ALPHA code were reformulated in strong conservation form by application of a Jacobian transformation to the equations in cylindrical polar coordinates, and a consistent technique for determination of the local time-dependent Jacobian determinant of the coordinate transformation was implemented. This particular formulation avoids mass sources associated with certain forms of the governing equations with moving coordinates.

The governing equations, constitutive relations and the time-dependent coordinate system developed herein have been incorporated into an existing computer code which solves the three-dimensional time-dependent compressible Navier-Stokes equations using a consistently split, linearized, block-implicit numerical scheme. The computer code developed under this effort has been designated as the ALPHA2 code.

UNCLASSIFIED

SECURITY CLASSIFICATION OF THIS PAGE(*When Data Entered*)

TABLE OF CONTENTS

	<u>Page</u>
INTRODUCTION.	5
THEORETICAL ANALYSIS.	8
Approach.	8
Governing Equations	9
Gas Phase Continuity	11
Solid Phase Continuity	11
Gas Phase Momentum	11
Solid Phase Momentum	11
Gas Phase Energy Equation.	12
Turbulence Kinetic Energy Equation	12
Gas Phase Mixture Molecular Weight and Specific Heat Equations	13
Particle Radius Equation	14
Interfacial Mass Transfer.	14
Stress Tensors	14
Heat Flux Vectors.	15
Mean Flow Dissipation.	16
Interfacial Energy Transfer.	16
Solid Phase Heat Conduction Equation	17
Constitutive Relations.	20
Gas Equation of State.	20
Molecular Viscosity, Bulk Viscosity, and Thermal Conductivity of Gas	21
Turbulence Model Relations	21
Turbulence Length Scale.	23
Interphase Turbulence Production	25
Form Functions	25
Intergranular Stress Relation.	26
Interphase Drag Relation	26
Interphase Heat Transfer Relation.	27
Burning Rate Correlation	28
Filler Element and Projectile Motion	28
Primer Discharge	30
COORDINATE TRANSFORMATION	31
SOLUTION PROCEDURE.	37
Initial and Boundary Conditions	39

TABLE OF CONTENTS (Continued)

	<u>Page</u>
REFERENCES.	43
APPENDIX.	47
LIST OF SYMBOLS	52
DISTRIBUTION LIST	57

INTRODUCTION

The flow and heat transfer in the projectile launching tube of a weapon is typically a complicated two-phase flow where combustion products are mixed with unburned propellant grains. A detailed calculation of the flow field in the gun tube would provide important information such as local transient heat transfer rates and propellant burning characteristics. This information would contribute to the understanding and solution of problems associated with gun barrel erosion and catastrophic gun failures. The present work is an extension in the development of the computer code ALPHA (Ref. 1) which solves the governing equations for the two-phase, two-dimensional flow in a gun tube.

Other efforts in modeling the flow phenomena in guns include quasi-one-dimensional inviscid two-phase flow analyses of the propellant combustion process (e.g., Ref. 2-7), a two-dimensional inviscid two-phase flow analysis (Ref. 8), and time-dependent boundary layer analyses applied to the flow of propellant gases in a gun tube (Refs. 9 and 10). The boundary layer procedures suffer from the shortcoming that the starting conditions near the projectile base are not well defined, and according to conventional boundary layer theory the heat flux near the base approaches infinity because the base is a singular point (Ref. 10). Furthermore, the validity of the boundary layer approximations is questionable at both the breech end and the projectile base region, and even the most sophisticated boundary layer analysis presently used for gun barrel problems, e.g., Refs. 9 and 10, did not consider the two-phase flow aspects of the propellant combustion process. The significant features of the two-phase flow interior ballistics codes (Refs. 2-7) were reviewed by Kuo (Ref. 11). The main objection to these analyses (Refs. 2-7) would seem to be the presumption of quasi-one-dimensional flow and the attempt to predict heat transfer to the barrel using rather simple unsteady boundary layer models or correlation formulas. The two-dimensional analysis of Gough (Ref. 8) utilizes an explicit two-step time-dependent algorithm due to MacCormack (Ref. 12) with upwind spatial differencing modifications suggested by Moretti (Ref. 13). The coordinate transformation technique used in Ref. 8 is based on the method of Thompson, et. al. (Ref. 14). The initial work of Ref. 8 considers only a stationary coordinate system to model the ignition process in a closed chamber with geometrical complications such as a hemispherical breech closure plug and a boattail projectile intrusion. According to Ref. 8, this stationary coordinate system

would be transformed to a moving system via a solid phase Lagrangian transformation so that the mesh moves with the particles. It is not known if this technique will give accurate results when projectile motion is included in the calculation. However, since the governing equations in Ref. 8 were written in nonconservation form, significant coordinate motion may give rise to mass sources due to time truncation error introduced by a moving mesh as demonstrated by Thomas and Lombard (Ref. 15). Furthermore, if the mesh motion is governed by the solid particle motion, inadequate resolution may result in certain areas of the computational domain. Finally, prediction of barrel heat transfer with an inviscid core flow analysis would require potentially inaccurate unsteady boundary layer models as in the quasi-one-dimensional analyses.

The complex nature of the flow in the projectile base region and in the breech end of the barrel does not permit simplifying approximations to be made in the governing fluid flow equations, and therefore in principle the solution of the full Navier-Stokes equations is required, rather than some simpler approximate set of equations. Fortunately, recent developments in computational fluid dynamics have made possible the prediction of the detailed flow field in configurations such as a gun barrel using the full Navier-Stokes equations. The equations and coordinate system developed under this effort have been incorporated into an existing three-dimensional time-dependent compressible Navier-Stokes calculation procedure (the MINT code) which was originally developed under United States Navy and Air Force sponsorship for other purposes by staff members of Scientific Research Associates, Inc. (Refs. 16-19). The MINT procedure solves the governing equations using a consistently-split, linearized, block-implicit numerical scheme (Ref. 20).

Under a previous effort (Ref. 1) a mathematical model of a two-phase, two-dimensional flow was developed and a computer code (ALPHA) was constructed for the numerical solution of the equations resulting from this mathematical model. The model developed consists of the governing equations for an axisymmetric, two-phase flow in a gun tube with a rotating projectile, and a system of constitutive relations describing the molecular viscosity and thermal conductivity, turbulence length scale, gas equation of state, intergranular stress, interphase drag, interphase heat transfer, and solid phase combustion. The governing equations and corresponding initial and boundary conditions described the firing cycle beginning with a fluidized and ignited solid phase, and ending with the

projectile exiting the gun tube. Chemical reactions within the gas phase were excluded from the formulation. An axisymmetric time-dependent adaptive coordinate system for interior ballistics flow field calculations was developed, and the projectile and distinct filler elements were treated using a quasi-one-dimensional lumped parameter analysis.

Under the present effort the ALPHA code has been modified to include both an ignition model to permit computation of the complete firing cycle and the capability to treat geometries in which the tube radius is a function of axial distance. An efficient procedure for mass storage and/or large core memory utilization for the ALPHA code dependent variable array and the block-tridiagonal matrix inversion array was implemented and made operational. Further, an existing SRA capability for velocity vector and contour plotting of ALPHA code output was made operational on the BRL computer system. The moving coordinate system capability in the previously developed ALPHA code (Ref. 1) was observed to have truncation error produced mass sources associated with the form of the governing equations utilized. This observation of truncation error produced by moving meshes is consistent with the findings of Thomas and Lombard (Ref. 15), who suggested reformulation of the governing equations in strong conservation form along with a special technique for determination of the local time-dependent Jacobian determinant of the coordinate transformation. Therefore, under the present effort the governing conservation equations were reformulated in a strong conservation form by application of a Jacobian transformation to the equations in cylindrical-polar coordinates. The resulting computer code has been designated as ALPHA2.

THEORETICAL ANALYSIS

Approach

The governing equations for a two-phase two-dimensional flow in a gun tube which were originally presented in vector form in Ref. 1 are repeated below for completeness. The provision for a rotating projectile is considered by solving the azimuthal momentum conservation equation with the appropriate boundary conditions at the projectile base. The governing equations may be obtained by employing either the time-averaging procedure utilized by Ishii (Ref. 21) or the formal averaging approach used by Gough (e.g., Refs. 22,23) or Gough and Zwarts (Ref. 24). In the present derivation, the averaging procedure of Gough (Ref. 22) has been selected because of its notational convenience; however, extensive reference to the work of Ishii (Ref. 21) has been made in order to verify the results obtained. In the following analysis, a gas-solid mixture is assumed with a constant solid phase density, ρ_p . Numerous assumptions and approximations are required in order to formulate a tractable problem. Most of the required assumptions have been stated previously by Gough (e.g., Ref. 2), and those necessary in the present work are:

- (1) The gas and solid phases occupy separate complementary regions, and within each region the material may be treated as a homogeneous continuum.
- (2) The flow of the heterogeneous mixture, composed of the two interacting continua, can be described by appropriately defined averages of the flow properties.
- (3) If solid phase combustion occurs, the energy deposition is taken to be in the gas only.
- (4) The solid phase is deformable and incompressible. However, locally no relative motion between the solid particles is considered. Thus the average stress in the solid phase is an isotropic normal stress.
- (5) The influence of solid phase deformation on the particle surface area is neglected, and the interfacial average of the particle velocity is equal to the volume average in the absence of burning.
- (6) The interphase drag is determined from steady state correlations; the unsteady virtual mass effect is not considered.
- (7) The interphase heat transfer is determined from steady state correlations.

- (8) The Noble-Abel equation of state is employed. The specific heats (c_p and c_v) are taken to be independent of temperature.
- (9) The regression rate of the surface of the burning propellant is a function of the average gas properties and the propellant surface temperature.
- (10) Heat transfer to the solid phase is treated as a one-dimensional process in order to determine the propellant surface temperature.
- (11) The pressure drop at the gas-solid interface is negligible.

Governing Equations

Both Ishii (Ref. 21) and Gough (Refs. 22, 23) have presented the relations for the average of time and space derivatives in a two-phase mixture. Using the above assumptions a system of partial differential equations is obtained containing interface-averaged source terms arising from averaging the basic conservation equations for the two-phase mixture. A basic quantity used to describe a two-phase mixture is the porosity, α , i.e., the ratio of volume occupied by the gas phase to the total volume. Ishii (Ref. 21) introduces several averages which are required in the present analysis. Gough (Ref. 22) introduces a general weighting function $g(\vec{y} - \vec{x}, \tau - t)$ which reflects the influence of remote points (\vec{y}, τ) on the average value at (\vec{x}, t) . By definition, the Gough average gives

$$\int_{\text{all } V, t} g(\vec{x}, t) d\vec{x} dt = 1 \quad (1)$$

The porosity is defined by

$$\alpha(\vec{x}, t) = \int_{V_{\text{gas}}} g(\vec{y} - \vec{x}, \tau - t) d\vec{y} d\tau \quad (2)$$

The weighting function, g , plays a role similar to the state density functions (M_1, M_2, M_s) introduced by Ishii (Ref. 21, p. 65). The basic time average introduced by Ishii (Ref. 21, p. 68) is denoted by a single overbar ($\bar{\psi}$), and this is equivalent to Gough's (Ref. 2) unnormalized average. The phase average

denoted by a double overbar ($\bar{\bar{\psi}}$) is related to $\bar{\psi}$ by

$$\bar{\bar{\psi}} = \frac{\bar{\psi}}{\alpha} = \frac{1}{\alpha} \int_{V_{gas}} g(\vec{y} - \vec{x}, \tau - t) \psi(\vec{y}, \tau) d\vec{y} d\tau \quad (3)$$

Eq. (3) defines the average of a gas property, ψ , since the integral is carried out over the region occupied by the gas phase, V_{gas} . In Ishii's approach the equivalent average is obtained by integrating only over the time interval for which the gas phase is present at the space point \vec{x} . Finally, the mass weighted average for a property of the k^{th} -phase ψ_k is defined by

$$\bar{\psi}_k^F = \frac{\bar{\rho}_k \psi_k}{\bar{\rho}_k} = \frac{\bar{\bar{\rho}}_k \bar{\bar{\psi}}_k}{\bar{\bar{\rho}}_k} \quad (4)$$

This average is also known as the Favré average, hence the superscript F is used. This is a very convenient average to use in turbulent flow since density fluctuations may be eliminated formally. It should be noted that the quantity $\bar{\rho}_k$ is the partial density of k^{th} -phase while $\bar{\bar{\rho}}_k$ is the actual density, so that the mixture density is given by

$$\bar{\rho}_m = \sum_{k=1}^2 \bar{\rho}_k = \sum_{k=1}^2 \alpha_k \bar{\rho}_k \quad (5)$$

where $\alpha_1 \equiv \alpha$, and $\alpha_2 \equiv 1-\alpha$.

In the following equations, the Favré average is introduced where it is appropriate, and phase average values are used otherwise. The Favré-averaged velocity vector is written as

$$\bar{\bar{U}}^F \equiv \bar{U} \quad (6)$$

and on all other variables (e.g., e , h , etc.) the superscript F is dropped for convenience. The fluctuating component of any variable is denoted with a superscript prime, ψ' . All quantities pertaining to the solid phase are denoted by the subscript p . The derivation of the equations is discussed in some detail in Ref. (1) and will not be repeated here. The resulting equations are

Gas Phase Continuity

$$\frac{\partial(\alpha \bar{\rho})}{\partial t} + \nabla \cdot (\alpha \bar{\rho} \vec{U}) = \Gamma_1 + \dot{M}_{ig} \quad (7)$$

Solid Phase Continuity

$$\frac{\partial(1-\alpha)}{\partial t} + \nabla \cdot [(1-\alpha) \vec{U}_p] = - \frac{\Gamma_1}{\rho_p} \quad (8)$$

where the mass source, Γ_1 , is due to propellant burning and \dot{M}_{ig} is the rate of mass addition due to primer discharge.

Gas Phase Momentum

$$\begin{aligned} \frac{\partial(\alpha \bar{\rho} \vec{U})}{\partial t} + \nabla \cdot (\alpha \bar{\rho} \vec{U} \vec{U}) &= - \alpha \nabla \bar{\rho} + \nabla \cdot [\alpha (\bar{\pi} + \pi^T)] \\ &- (1-\alpha) \frac{S_p}{V_p} \langle \vec{F} \rangle^i + \vec{U}_p \Gamma + \dot{M}_{ig} \vec{U}_{ig} \end{aligned} \quad (9)$$

Solid Phase Momentum

$$\begin{aligned} \frac{\partial[(1-\alpha) \rho_p \vec{U}_p]}{\partial t} + \nabla \cdot [(1-\alpha) \rho_p \vec{U}_p \vec{U}_p] &= - (1-\alpha) \nabla \bar{\rho} \\ &+ \nabla \cdot [(1-\alpha) \mathbf{R}] + (1-\alpha) \frac{S_p}{V_p} \langle \vec{F} \rangle^i - \vec{U}_p \Gamma \end{aligned} \quad (10)$$

In the above equations, $\bar{\pi}$ and π^T are the average stress tensor and the turbulent stress tensor in the gas phase, respectively, $\bar{\bar{R}}$ is the average granular stress tensor, and π_p^T is the solid phase turbulent stress tensor. For the present time π_p^T will be neglected because there is insufficient information available to construct a constitutive relation for it. The quantity \vec{F}^i is the interfacial drag force and \vec{U}_{ig} is the primer gas velocity.

Gas Phase Energy Equation

In the present formulation it is desirable to write the energy equation in terms of the mass-averaged static enthalpy \bar{h} because of simplifications in the turbulence time-averaging.

$$\begin{aligned} \frac{\partial(\alpha \bar{\rho} \bar{h})}{\partial t} + \nabla \cdot (\alpha \bar{\rho} \vec{U} \bar{h}) &= - \nabla \cdot \left[\alpha (\bar{\bar{q}} + \bar{q}^T) \right] \\ + \frac{D}{Dt} (\alpha \bar{\rho}) + \alpha \bar{\Phi} + \alpha \bar{\rho} \bar{\epsilon} + \Lambda + \dot{M}_{ig} \left(h_{ig} + \frac{1}{2} \vec{U}_{ig} \cdot \vec{U}_{ig} \right) \end{aligned} \quad (11)$$

where Φ is the mean flow dissipation defined in Eq. (28), $\bar{\epsilon}$ is the turbulence kinetic energy dissipation rate, Eq. (50), h_{ig} is the enthalpy of the primer gas, and Λ is the energy transfer term between the solid and gas phases, Eq. (29).

Turbulence Kinetic Energy Equation

In the present work a turbulence kinetic energy equation and a specified length scale equation has been utilized. Following the derivations of Refs. (25-26) and Ref. (1), one obtains

$$\begin{aligned} \frac{\partial(\alpha \bar{\rho} \bar{k})}{\partial t} + \nabla \cdot (\alpha \bar{\rho} \vec{U} \bar{k}) &= \nabla \cdot \left(\alpha \frac{\mu_T}{\sigma_k} \nabla \bar{k} \right) \\ + \alpha \left\{ \mu_T \left[2 \mathbb{D} : \mathbb{D} - \frac{2}{3} (\nabla \cdot \vec{U})^2 \right] - \frac{2}{3} \bar{\rho} \bar{k} \nabla \cdot \vec{U} - \bar{\rho} \bar{\epsilon} \right\} + s_k \end{aligned} \quad (12)$$

where S_k is an interphase turbulence production term, Eq. (68), and \bar{k} is the mean gas phase turbulence kinetic energy

$$\bar{k} = \frac{1}{2} \overline{\vec{U}' \cdot \vec{U}'} \quad (13)$$

Gas Phase Mixture Molecular Weight and Specific Heat Equations

In the present two-phase flow analysis the gas phase species and gasified propellant species mass fractions are not required. Therefore, in order to limit computer requirements the individual species mass conservation equations are not solved, but rather only total gas and solid phase continuity equations are solved. Therefore, it is necessary to consider transport equations for the inverse mixture molecular weight (Z) and the specific heat at constant pressure (c_p):

$$\frac{\partial}{\partial t} (\alpha \bar{\rho} Z) + \nabla \cdot (\alpha \bar{\rho} \vec{U} Z) = \nabla \cdot [\alpha \Gamma_m \nabla Z] + Z_p \Gamma \quad (14)$$

where Γ_m is the turbulent exchange coefficient for species diffusion which is defined from a knowledge of the Schmidt number in the turbulent flow of gas mixtures,

$$\Gamma_m = \frac{\mu_{\text{eff}}}{Sc_{\text{eff}}} \quad (15)$$

and Sc_{eff} is generally taken as a constant, $Sc_{\text{eff}} = 0.9$. The effective viscosity, μ_{eff} , is defined by Eq. (56). Further, Z_p is the inverse molecular weight of the propellant and Γ is the mass source due to propellant burning, Eq. (18).

A similar transport equation may be derived for the specific heat by assuming that the species specific heats are independent of temperature:

$$\frac{\partial (\alpha \bar{\rho} c_p)}{\partial t} + \nabla \cdot (\alpha \bar{\rho} \vec{U} c_p) = \nabla \cdot [\alpha \Gamma_m \nabla c_p] + (c_p)_p \Gamma \quad (16)$$

where $(c_p)_p$ is the specific heat at constant pressure of the propellant.

Particle Radius Equation

The average particle radius, r_p , is required as a function of spatial location and time for the constitutive relations specified below. The appropriate equation including turbulent diffusion is

$$\begin{aligned} & \frac{\partial[(1-\alpha)\rho_p r_p]}{\partial t} + \nabla \cdot \left[(1-\alpha)\rho_p \vec{U}_p r_p \right] \\ &= \nabla \cdot \left[(1-\alpha)\Gamma_m \nabla r_p \right] - (1-\alpha)\rho_p \left(1 + r_p \frac{S_p}{V_p} \right) \langle \dot{d} \rangle^i \end{aligned} \quad (17)$$

where the relation for Γ , Eq. (18), has been incorporated in order to cast the equation for the average particle radius r_p into the above form.

Interfacial Mass Transfer

Following Ref. (22), the mass source due to propellant burning may be written

$$\Gamma = (1-\alpha) \frac{S_p \rho_p}{V_p} \langle \dot{d} \rangle^i \quad (18)$$

where S_p is the average particle surface area, V_p is the average particle volume, and $\langle \dot{d} \rangle^i$ is the average regression rate of the solid phase, Eq. (79).

Stress Tensors

The gas phase stress tensor assuming a Newtonian fluid is

$$\bar{\pi} = 2\mu \mathbb{D} - \left(\frac{2}{3} \mu - K_B \right) \nabla \cdot \vec{U} \mathbb{I} \quad (19)$$

where K_B is the bulk viscosity coefficient and \mathbb{D} is the total deformation tensor (or rate of strain tensor) given by (Ref. 21, p. 164)

$$\mathbb{D} = \mathbb{D}_b + \mathbb{D}_i \quad (20)$$

where \mathbb{D}_b is the bulk deformation tensor,

$$\mathbb{D}_b \equiv \frac{1}{2} \left[(\nabla \vec{U}) + (\nabla \vec{U})^T \right] \quad (21)$$

and \mathbb{D}_i is the interfacial deformation tensor which is difficult to model except for a dispersed flow (Ref. 21, p. 165), hence it must be neglected at present. The turbulent flow stress tensor in the gas phase is modeled using an isotropic eddy viscosity formulation, i.e.,

$$\pi^T = -\bar{\rho} \overline{\vec{U}' \vec{U}'} = 2\mu_T \mathbb{D} - \frac{2}{3} (\mu_T \nabla \cdot \vec{U} + \bar{\rho} \bar{k}) \mathbb{I} \quad (22)$$

where \bar{k} is the turbulence kinetic energy, Eq. (13). The turbulent viscosity μ_T must be determined using a suitable turbulence model. The solid phase granular stress tensor, \mathbb{R} , is modeled by assuming an isotropic normal stress, i.e.,

$$\mathbb{R} \equiv R_p \mathbb{I} \quad (23)$$

hence in the solid phase momentum Eq. (10),

$$\nabla \cdot \left[(1-\alpha) \mathbb{R} \right] = \nabla \left[(1-\alpha) R_p \right] \quad (24)$$

Heat Flux Vectors

The mean heat flux vector \vec{q} and the turbulent heat flux vector \vec{q}^T in a two-phase flow may be written as (Ref. 21, p. 165)

$$\vec{q} = -\bar{\kappa} \left[\nabla \bar{T} - \frac{\nabla \alpha}{\alpha} (\bar{T}_i - \bar{T}) \right] \quad (25)$$

and

$$\vec{q}^T = -\bar{\kappa}^T \left[\nabla \bar{\bar{T}} - \frac{\nabla a}{a} (\bar{\bar{T}}_i - \bar{\bar{T}}) \right] \quad (26)$$

where $\bar{\bar{\kappa}}$ is the mean thermal conductivity, Eq. (48), $\bar{\kappa}^T$ is a turbulent conductivity, Eq. (57), and $\bar{\bar{T}}_i$ is the mean temperature at the interface between the phases. For the present time $\bar{\bar{T}}_i$ will be taken as the average between the gas temperature and the particle surface temperature, i.e.

$$\bar{\bar{T}}_i = \frac{1}{2} (\bar{T} + \bar{\bar{T}}_{ps}) \quad (27)$$

and $\bar{\bar{T}}_{ps}$ will be determined from the solid phase heat conduction model.

Mean Flow Dissipation

The mean flow dissipation term appearing in the energy equation, Eq. (11), is defined as

$$\Phi = 2\mu \mathbb{D} : \mathbb{D} - \left(\frac{2}{3} \mu - K_B \right) (\nabla \cdot \vec{U})^2 \quad (28)$$

Interfacial Energy Transfer

Following Gough (Ref. 22), it can be shown that the interfacial energy transfer term in Eq. (11) is

$$\begin{aligned} \Lambda &= -\bar{\bar{p}} (\vec{U} - \vec{U}_p) \cdot \nabla a \\ &+ (1-a) \frac{S_p}{V_p} (\vec{U} - \vec{U}_p) \cdot \langle \vec{F} \rangle^i + \bar{\bar{q}} \cdot \nabla a \\ &- (1-a) \frac{S_p}{V_p} \langle q \rangle^i + \Gamma \left[h_{comb} + \frac{1}{2} (\vec{U} - \vec{U}_p) \cdot (\vec{U} - \vec{U}_p) \right] \end{aligned} \quad (29)$$

where $\langle q \rangle^i$ is the interfacial average heat transfer between the gas and solid phases, Eq. (78), and h_{comb} is the energy released (per unit mass) due to

combustion of the solid propellant.

Further details on the derivation of the interphase transfer terms in Eqs. (7-17) may be found in Refs. (21-22), and a summary is given in Ref. 1. In the present analysis Eqs. (7-17) are solved in conjunction with Eqs. (18-29) and the constitutive relations for $\langle \dot{d} \rangle^i$, $\langle \dot{F} \rangle^i$, $\langle q \rangle^i$, μ , μ_T , K_B , $\bar{\kappa}$ and κ^T , which are given in a subsequent section.

Solid Phase Heat Conduction Equation

Since the solid particle surface temperature is desired to determine ignition, the propellant burning rate, and the rate of heat transfer between the gas and solid phase, a transient heat conduction equation must be solved. Gough (Ref. 2) and Kuo, et al., (Ref. 4) assume that the penetration depth of a thermal wave into the propellant grains is small compared to the grain dimensions. Then it is permissible to use a one-dimensional approximation (planar for cord propellant or spherical for spherical propellant grains) to obtain the particle surface temperature. Following the motion of a given particle (Kuo, et al., Ref. 4), the heat conduction equation for a spherical particle is

$$\left(\frac{d\bar{\bar{T}}_p}{dt} \right)_{\tilde{r}} = \frac{\alpha_p}{\tilde{r}^2} \frac{\partial^2 (\tilde{r}^2 \bar{\bar{T}}_p)}{\partial \tilde{r}^2} \quad (30)$$

where $\bar{\bar{T}}_p = \bar{\bar{T}}_p(\tilde{r}; \vec{x}, t)$ is the phase-averaged temperature within a representative particle, \tilde{r} is radial coordinate within the particle, α_p is the thermal diffusivity of the solid particles [$\alpha_p = k_p / \rho_p c_p$], and $(d/dt)_{\tilde{r}}$ denotes the Lagrangian time derivative at constant \tilde{r} within the particle. Since the surface of a representative burning particle is receding in time it is desirable to employ the following time-dependent transformation for the particle radial coordinate \tilde{r} :

$$\zeta \equiv \frac{\tilde{r}}{r_p(t)} ; \quad 0 \leq \zeta \leq 1 \quad (31)$$

Then Eq. (30) becomes,

$$\left(\frac{d\bar{\bar{T}}_p}{dt} \right)_{\zeta} - \left(\frac{\zeta}{r_p} \frac{dr_p}{dt} \right) \frac{\partial \bar{\bar{T}}_p}{\partial \zeta} = \frac{\alpha_p}{\zeta^2 r_p^2} \frac{\partial^2}{\partial \zeta^2} (\zeta^2 \bar{\bar{T}}_p) \quad (32)$$

where the quantity

$$R_s \equiv - \frac{dr_p}{dt} = \langle \dot{d} \rangle^i \quad (33)$$

may be identified as the average surface regression rate for the particle, $R_s \geq 0$.

The initial condition for Eq. (32) is

$$\bar{\bar{T}}_p(\zeta, t=0) = \bar{\bar{T}}_{po} \quad (34)$$

The boundary conditions are

$$\frac{\partial \bar{\bar{T}}_p}{\partial \zeta}(\zeta=0, t) = 0 \quad \text{at} \quad \zeta=0 \quad (35)$$

$$\frac{k_p}{r_p} \frac{\partial \bar{\bar{T}}_p}{\partial \zeta}(\zeta=1, t) = h_c(t) \left[\bar{\bar{T}} - \bar{\bar{T}}_{ps} \right] + q_{rad} + k_p \phi(R_s, p) \quad \text{at} \quad \zeta=1 \quad (36)$$

where q_{RAD} is the net incident radiation heat flux normal to the particle surface, k_p is the thermal conductivity of the solid particles, and $\phi(R_s, p)$ is the heat feedback from the flame identified by Gough (Ref. 2, p. 57). Assuming that the gas is nearly in radiative equilibrium so that the gas emissivity is unity, and that radiation emitted by other particles does not influence the particle in question, we obtain

$$q_{rad} = \epsilon_p \sigma \left(\bar{\bar{T}}^4 - \bar{\bar{T}}_{ps}^4 \right) \quad (37)$$

where ϵ_p is the particle emissivity. Other authors (e.g., Refs. 2-4) have cast Eq. (37) into a heat transfer coefficient form, so Eq. (36) becomes

$$\frac{k_p}{r_p} \frac{\partial \bar{T}_p}{\partial \zeta} (\zeta = 1, t) = h_t(t) [\bar{T} - \bar{T}_{ps}] + k_p \phi(R_s, p) \quad (38)$$

where the total heat transfer coefficient is

$$h_t = h_c + \epsilon_p \sigma (\bar{T} + \bar{T}_{ps}) (\bar{T}^2 + \bar{T}_{ps}^2) \quad (39)$$

The convective heat transfer coefficient, h_c , is specified via a constitutive relation, Eq. (77). An expression for $\phi(R_s, p)$ has been presented by Gough (Ref. 2) for a planar geometry under the assumption that the flame zone surrounding the burning particle remains quasi-steady, and that the convection and radiation heat transfer terms in Eq. (36) are zero. It then follows that

$$\phi = \frac{R_s}{\alpha_p} (\bar{T}_{ps} - \bar{T}_{po}) \quad (40)$$

where α_p is the thermal diffusivity of the particles and \bar{T}_{po} is the undisturbed temperature far from the particle surface. In the context of spherical particles, \bar{T}_{po} would be taken as the temperature at the center of the particle. This procedure should be sufficiently accurate in view of the other assumptions made in obtaining Eq. (40).

In the ALPHA2 code, Eqs. (34-37, 40) have been utilized. Solution of this solid phase heat conduction model requires special consideration since it is in Lagrangian form, whereas all other differential conservation equations are in Eulerian form. The method to be employed in the present analysis will be described in the section on Solution Procedure.

Constitutive Relations

The necessary constitutive relations include a gas phase equation of state, a caloric equation of state, a turbulence length scale distribution, the molecular viscosity and thermal conductivity, the so-called form functions for the surface area and volume of the solid particles, an intergranular stress relation, interphase drag and heat transfer relations, and a burning rate correlation for the solid phase combustion. In the following, the double overbar () is dropped for simplicity.

Gas Equation of State

The Nobel-Abel equation of state will be used for the gas,

$$\rho(1-\rho\eta) = \frac{\rho R_u T}{w_m} \equiv \rho Z T \quad (41)$$

where R_u is the universal gas constant, w_m is the gas molecular weight, and η is the covolume factor, which is composition dependent. Following Gough (Ref. 2) an arithmetic average will be used for η based upon the propellant properties.

The caloric equation of state is taken as

$$e = c_v T \quad (42)$$

where c_v is dependent on the gas composition but not temperature. The static enthalpy is then

$$h = e + \frac{p}{\rho} = c_v T + \frac{Z T}{1-\eta\rho} \quad (43)$$

The specific heat at constant pressure is

$$c_p \equiv \left. \frac{\partial h}{\partial T} \right|_p = c_v + Z \quad (44)$$

so that Eq. (43) may be written as

$$h = c_p T + \eta p \quad (45)$$

Molecular Viscosity, Bulk Viscosity, and Thermal Conductivity of Gas

The molecular viscosity for the gas is determined from Sutherland's law,

$$\frac{\mu}{\mu_0} = \left(\frac{T}{T_0} \right)^{3/2} \frac{T_0 + S_1}{T + S_1} \quad (46)$$

where $S_1 = 110^\circ\text{K}$ for air.

The bulk viscosity for the gas will be assumed to be zero at present,

$$\kappa_B = 0 \quad (47)$$

The thermal conductivity may be determined from a relation similar to Sutherland's law, e.g.,

$$\frac{\kappa}{\kappa_0} = \left(\frac{T}{T_0} \right)^{3/2} \frac{T_0 + S_2}{T + S_2} \quad (48)$$

where $S_2 = 194^\circ\text{K}$ for air.

Turbulence Model Relations

The turbulent viscosity introduced in Eq. (22) is obtained from the Prandtl-Kolmogorov relation, viz.

$$\mu_T = c_\mu \frac{\bar{\rho} \bar{k}^2}{\bar{\epsilon}} \quad (49)$$

and the dissipation rate is given by

$$\bar{\epsilon} = c_\mu^{3/4} \frac{\bar{k}^{3/2}}{\ell} \quad (50)$$

where the turbulence length scale, ℓ , must be specified consistent with the expected turbulence structure in the two-phase flow. Following Ref. 27 the constant σ_k will be taken as

$$\sigma_k = 1.0 \quad (51)$$

The very large fluid accelerations experienced in the interior ballistics problem require the consideration of both forward and reverse transition of

the turbulent flow near solid surfaces. There are two options available for modeling the turbulence near a wall. In the first, grid point resolution normal to the wall must be sufficient to define the viscous sublayer, in which case the boundary conditions are relatively straightforward. However, the difficulty with this approach is that the physics of low Reynolds number (transitional) turbulence must be modeled in a reasonable manner by the governing turbulence equations (e.g., Jones and Launder, Ref. 27). An alternative approach is to employ a less refined mesh and force the turbulence variables to yield values consistent with a boundary layer wall function formulation at the first grid point away from the wall. The difficulty with this approach is that the validity of the wall function formulation is questionable under the rapidly accelerating transient flow situation present in the interior ballistics problem. Furthermore, recent experience at SRA indicates that the wall function approach may be inadequate for a reacting unsteady flow with moving coordinates. Therefore, a transition model, which was successfully used by Shamroth and Gibeling (Ref. 28) in a time dependent airfoil flow field analysis, has been implemented in the computer code. The analysis of Ref. 28 follows the integral turbulence energy procedure of Refs. 29-31, by utilizing a turbulence function a_1 , where

$$a_1 = C_\mu^{1/2} / 2 \quad (52)$$

and a_1 is taken as a function of a turbulence Reynolds number of the form

$$a_1 = a_0 \left[\frac{f(R_\tau)}{100} \right] / \left\{ 1.0 + 6.66 a_0 \left[\frac{f(R_\tau)}{100} - 1 \right] \right\} \quad (53)$$

where

$$a_0 = .0115$$

$$f(R_\tau) = 100 \cdot R_\tau^{0.22} \quad R_\tau \leq 1 \quad (54)$$

$$f(R_\tau) = 68.1 R_\tau + 614.3 \quad R_\tau \geq 40$$

and a cubic curve was fit for values of R_τ between 1 and 40. As previously discussed, Ref. 29-31 utilized an integral form of the turbulence kinetic energy and therefore R_τ was defined as an average value.

$$R_T = \frac{1}{\delta} \int_0^\delta \nu_T dy / \frac{1}{\delta} \int_0^{\delta_s} \nu dy_s \quad (55)$$

In the present effort R_T was defined as the local ratio of turbulent to laminar viscosity, a_1 was evaluated via Eq. 53 and C_μ related to a_1 via Eq. 52.

The effective viscosity is defined as the sum of the laminar and turbulent viscosities

$$\mu_{\text{eff}} = \mu + \mu_T \quad (56)$$

The effective conductivity will be modeled using an effective Prandtl number obtained from knowledge of turbulent flows of gases and gas mixtures, i.e.,

$$\kappa_{\text{eff}} \equiv \bar{\kappa} + \kappa^T = \frac{c_p \mu_{\text{eff}}}{Pr_{\text{eff}}} \quad (57)$$

and $Pr_{\text{eff}} = 0.9$ for air.

Turbulence Length Scale

For the evaluation phase of the present effort, the turbulence length scale would be chosen based upon known steady state relations. In particular, the length scale would be taken as the minimum of the length scales based upon the local average distance between solid particles, the local value computed from turbulent pipe flow correlations, and that from turbulent boundary layer length scale distributions when close to the wall.

The turbulent pipe flow mixing length model is based on the correlation of Williamson (Ref. 32),

$$\frac{\ell_M^T}{r_1} = C_w \left(\frac{y}{r_1} \right) \exp \left(1 - \frac{y}{r_1} \right) \quad (58)$$

where r_1 is the local pipe radius, y is the distance from the point in question to the nearest wall, and the constant C_w is taken as

$$C_w = 0.14 \quad (59)$$

The near wall region mixing length is obtained from the Van Driest model (Ref. 33),

$$\ell_w^T = \kappa y \left[1 - \exp(-y^+/A^+) \right] \quad (60)$$

where κ is the von Karman constant and A^+ is the van Driest damping coefficient,

$$\kappa = 0.4 \quad (61)$$

$$A^+ = 26.0$$

The nondimensional distance y^+ is defined as

$$y^+ = y \left(\frac{\rho U_\tau}{\mu} \right) \quad (62)$$

and the friction velocity u_τ in the present analysis is taken as

$$U_\tau = \left(\frac{\tau_\ell}{\rho} \right)^{1/2} \quad (63)$$

where the local shear stress τ_ℓ is obtained from

$$\tau_\ell = (2D/D)^{1/2} \quad (64)$$

The average center to center distance between solid spherical particles assuming dense packing is approximately

$$\ell_c \simeq \left(\frac{V_p}{1-a} \right)^{1/3} \quad (65)$$

Therefore, the minimum distance between particle surfaces is

$$\ell_p = \ell_c - 2r_p \quad (66)$$

and the turbulence length scale will be assumed proportional to the distance ℓ_p , viz.

$$\ell_p^T = \beta_p \ell_p \quad (67)$$

The constant β_p should be selected based upon empirical observation of the turbulence structure in two-phase flows with solid particles.

Interphase Turbulence Production

The interphase turbulence production term S_k in Eq. (12) may be interpreted as the production of turbulence kinetic energy in the gas phase due to gasification of solid particles (Ref. 1),

$$S_k \approx \bar{k}_{ps} \Gamma \quad (68)$$

where \bar{k}_{ps} represents an average value for $1/2 (\vec{u}' \cdot \vec{u}')$ at the gas-solid interface. It is not known how to specify \bar{k}_{ps} at the present time, and consequently until further information becomes available $\bar{k}_{ps} = 0$.

Form Functions

The surface area and volume of particles have been presented by Gough (Ref. 2) for a variety of propellant types. In the present work, spherical propellant grains will be considered, hence

$$V_p = \frac{4}{3} \pi r_p^3$$
$$S_p = 4 \pi r_p^2 \quad (69)$$

where r_p is the mean particle radius at a given point in space and time. Other propellant types could easily be considered within the present framework.

Intergranular Stress Relation

A stress relation for granular propellant has been given by Gough (Ref. 2), Koo and Kuo (Ref. 3), and Kuo, et al., (Ref. 4) for the case when the average stress R_p is independent of the loading history:

$$R_p = \begin{cases} -\rho_p a_p^2 \frac{\alpha_c - \alpha}{(1 - \alpha)} \frac{\alpha_c}{\alpha} & \text{if } \alpha \leq \alpha_c \\ 0 & \text{if } \alpha > \alpha_c \end{cases} \quad (70)$$

where α_c is a critical porosity above which there is no direct contact between particles, and a_p is the speed of sound in the solid phase specified on input.

Interphase Drag Relation

The average steady state interphase drag $\langle \vec{F} \rangle^i$ appearing in the momentum equations, Eq. (9-10), was obtained from correlations for nonfluidized (packed) regions and fluidized (dispersed) regions. Gough (Ref. 2, p. 48) recommended the following drag correlation, valid for high particle Reynold's numbers, $Re_p \gg 1$, which is based on Ergun's (Ref. 34) correlation for a packed bed and modified by Anderssen's correlation (Ref. 35) as the bed becomes dispersed.

$$\langle \vec{F} \rangle^i = \frac{\rho \vec{U}_R |\vec{U}_R|}{6} f \quad (71)$$

with

$$f = \begin{cases} 1.75 & \alpha \leq \alpha_c \\ 1.75 \left[\frac{1 - \alpha}{1 - \alpha_c} \frac{\alpha_c}{\alpha} \right]^{0.45} & \alpha_c < \alpha \leq \alpha_1 \\ 0.3 & \alpha_1 < \alpha \leq 1 \end{cases} \quad (72)$$

where α_c is the settling porosity and α_1 is given by

$$\alpha_1 = \left[1 + 0.01986 \left(\frac{1 - \alpha_c}{\alpha_c} \right) \right]^{-1} \quad (73)$$

Also, \vec{U}_r is the relative velocity between the gas and solid phases, i.e.,

$$\vec{U}_R = \vec{U} - \vec{U}_P \quad (74)$$

and the particle Reynold's number is

$$Re_p = \frac{2r_p \rho |\vec{U}_R|}{\mu} \quad (75)$$

Gough (Ref. 8) has noted the potential source of error due to the presence of relatively few propellant grains in the radial direction of a typical medium caliber weapon (15-20 cm. diameter), since the available correlations are based on flows through long columns where end effects are negligible.

Interphase Heat Transfer Relation

For convective heat transfer between the gas and solid particles in interior ballistics calculations, numerous correlations have been recommended (e.g., Refs. 2-4, 7). Gough (Ref. 2) advocates the Gelperin-Einstein correlation (Ref. 36) for the interphase heat transfer with granular propellant in both fluidized and nonfluidized regions. The Nusselt number for this correlation is (Ref. 2)

$$Nu_p = 2.0 + 0.4 Re_p^{2/3} Pr^{1/3} \quad (76)$$

where $Pr = \frac{\mu c_p}{\kappa}$ and κ is the gas phase thermal conductivity, Eq. (48). The heat transfer coefficient in Eq. (36) is then

$$h_c = \frac{\kappa}{2r_p} Nu_p \quad (77)$$

This relation is considerably simpler than the Denton and Rowe-Claxton correlations utilized by Kuo, et al. (e.g., Refs. 3, 4), and may yield equally reliable predictions in view of the large variations between experimental data and the existing correlations (Ref. 2).

Finally, the interphase heat transfer relation required in the energy equation source term, Eq. (29), is

$$\langle q \rangle^i = h_t (\bar{T} - \bar{T}_{ps}) \quad (78)$$

where h_t is given by Eq. (39).

Burning Rate Correlation

The steady state surface regression rate ($d > 0$) is given by (e.g., Ref. 2)

$$\dot{d}_s = B_1 + B_2 p^n \quad (79)$$

where B_1 , B_2 and n have known constant values. The phenomenon of erosive burning is assumed to be an acceleration of the burning rate due to the influence of convective heat transfer on the heat transfer in the flame zone. The Lenoir-Robillard (Ref. 37) regression rate expression is utilized for this effect,

$$\dot{d}_E = \dot{d}_s + K_E h_c \exp \left[- \frac{\beta_E \rho_p \dot{d}_E}{\rho I U_R} \right] \quad (80)$$

where K_E and β_E are erosive burning constants, determined experimentally. The convective heat transfer coefficient is then obtained from Eqs. (77, 78). At present only the steady state burning relation, Eq. (79), has been incorporated into the computer code.

Filler Element and Projectile Motion

In the present analysis filler elements and the projectile are treated distinctly. No transverse deformation of the filler elements is permitted and elements are assumed to remain planar; therefore, a quasi-one-dimensional lumped parameter formulation (e.g., Ref. 2) may be employed for the filler elements. The appropriate equations, which have been stated by Gough (Ref. 2) are repeated here for completeness. It is assumed that there are N filler elements between propellant bed and the base of the projectile, with the projectile denoted as element ($N+1$). The required properties for each element are the mass (M_i), the resistance force opposing motion (F_i), an internal stress (σ_i), and a normal wall reaction force (F_{wi}) for incompressible elements in a variable area tube. The cross-sectional area of each element is assumed to be equal to the local tube area, and the stress in an incompressible element is assumed to be isotropic.

A momentum equation is then written for one-half of element i together with one-half of element ($i-1$) in order to describe the motion of the interface location, z_i . There results

$$\frac{1}{2} M_i \ddot{z}_i = A_i \sigma_i - A_0 \sigma_0 - \frac{F_i}{2} - \frac{F_{wi}}{2} \quad (81)$$

$$\frac{1}{2} (M_{i-1} + M_i) \ddot{z}_i = A_i \sigma_i - A_{i-1} \sigma_{i-1} - \frac{1}{2} (F_i + F_{i-1}) - \frac{1}{2} (F_{w_i} + F_{w_{i-1}}) \quad \text{for } 2 \leq i \leq N \quad (82)$$

$$\left(M_{N+1} + \frac{M_N}{2} \right) \ddot{z}_{N+1} = - A_N \sigma_N - \left(F_{N+1} + \frac{F_N}{2} \right) - \frac{F_{w_N}}{2} \quad (83)$$

In this section the stress σ_i is taken as positive in tension following Gough (Ref. 2), and the term $(-A_0 \sigma_0)$ in Eq. (81) is the force exerted on the first filler element by the gas and propellant particles. The mass of the projectile M_{N+1} is assumed to be corrected for rotational inertia; if I , D_B and θ are the polar moment of inertia, the tube diameter and the angle of rifling, respectively, it follows that

$$M_{N+1} = (M_{N+1})_{\text{actual}} + \frac{4I}{D_B^2} \tan^2 \theta \quad (84)$$

The normal wall reaction is given by

$$F_{w_i} = \begin{cases} 0 & \text{if element } i \text{ is not incompressible} \\ (z_{i+1} - z_i) \sigma_i \left(\frac{dA}{dz} \right)_i & \text{if element } i \text{ is incompressible} \end{cases} \quad (85)$$

Constitutive data must be provided for the stress σ_i for elastic elements or for plastic elements in a state of loading (i.e., $\dot{z}_i > \dot{z}_{i+1}$); however, for rigid elements or plastic elements in a state of unloading ($\dot{z}_i \leq \dot{z}_{i+1}$), one has

$$\sigma_i = 0, \dot{z}_i = \dot{z}_{i+1} \quad (86)$$

Finally, for an incompressible element, i , one has the continuity relation,

$$A_i \dot{z}_i = A_{i+1} \dot{z}_{i+1} \quad (87)$$

Primer Discharge

The primer discharge model is implemented as an external source of mass, momentum and energy into the gas phase in order to ignite the propellant grains. The general functional form of these source terms is

$$\dot{M}_{ig} = \dot{M}_{ig}(\bar{x}_i, t)$$

$$\vec{U}_{ig} = \vec{U}_{ig}(\bar{x}_i, t) \quad (88)$$

$$h_{ig} = h_{ig}(\bar{x}_i, t)$$

In practice the primer source is added only in a small region near either the tube centerline for a center core igniter or the breech end for a base igniter.

COORDINATE TRANSFORMATION

The set of governing partial differential equations which model the physical processes occurring in interior ballistics problems was presented in the previous section. For generality these equations were written in vector notation; however, before these equations can be incorporated into a computer code, a coordinate system must be chosen. The governing equations can then be cast in a form reflecting the choice of the coordinate system. The coordinate system for interior ballistics calculations must have the ability to enlarge the physical extent of the computational domain as the projectile moves through the gun barrel, and it must be capable of treating breech geometries in which the tube radius is a function of axial distance. Also, a time-dependent transformation is required to adapt the computational mesh to regions of large radial gradients appearing during the ignition phase of the firing cycle. The form of the governing equations appearing in Ref. 1 produces mass sources due to time truncation error when radial mesh motion is included in the calculation. This observation is consistent with the findings of Thomas and Lombard (Ref. 15), and appears to be due to an inconsistent calculation of the overall transformation Jacobian in the nonconservation form of equations (Ref. 1).

In order to permit consistent calculation of the Jacobian in a moving coordinate system, the governing equations should be transformed with a Jacobian transformation of the form

$$y^j = y^j(\bar{x}_1, \bar{x}_2, \bar{x}_3, t) \quad (89)$$

$$\tau = t$$

where $(\bar{x}_1, \bar{x}_2, \bar{x}_3) = (r, \theta, z)$ are the original cylindrical polar coordinates suitable for a gun tube. The velocity components remain the components, (u_1, u_2, u_3) in the $(\bar{x}_1, \bar{x}_2, \bar{x}_3)$ coordinate directions respectively. The new independent variables y^j are the computational coordinates in the transformed system. The coordinate system requirements for interior ballistics applications may be represented by a subset of the general transformation, Eq. (89),

$$y^1 = y^1(\bar{x}_1, \bar{x}_3, t) \quad (90a)$$

$$y^2 = y^2(\bar{x}_2) \quad (90b)$$

$$y^3 = y^3(\bar{x}_1, \bar{x}_3, t) \quad (90c)$$

which is a general axisymmetric time-dependent transformation. For interior ballistics flows which are axisymmetric, Eq. (90b) reduces to $y^2 = \bar{x}_2$ and all derivatives $\partial/\partial y^2$ are assumed to be zero. The transformation (90) with the axisymmetric flow assumption has been utilized in the ALPHA2 computer code.

Application of the Jacobian transformation requires expansion of the temporal and spacial derivatives using the chain rule, i.e.,

$$\frac{\partial \phi}{\partial t} = \frac{\partial \phi}{\partial \tau} + \sum_{j=1}^3 y_{,t}^j \frac{\partial \phi}{\partial y^j} \quad (91)$$

and

$$\frac{\partial \phi}{\partial \bar{x}_i} = \sum_{j=1}^3 y_{,i}^j \frac{\partial \phi}{\partial y^j} \quad (92)$$

where

$$\begin{aligned} y_{,t}^j &\equiv \frac{\partial y^j}{\partial t} \\ y_{,i}^j &\equiv \frac{\partial y^j}{\partial \bar{x}_i} \end{aligned} \quad (93)$$

The relations Eq. (91-93) are first substituted into the governing equations (7-17) written in cylindrical polar coordinates. Then the resulting equations are multiplied by the Jacobian determinant of the inverse transformation,

$$J = \frac{\partial(\bar{x}_1, \bar{x}_2, \bar{x}_3)}{\partial(y^1, y^2, y^3)} = \begin{vmatrix} \frac{\partial \bar{x}_1}{\partial y^1} & \frac{\partial \bar{x}_1}{\partial y^2} & \frac{\partial \bar{x}_1}{\partial y^3} \\ \frac{\partial \bar{x}_2}{\partial y^1} & \frac{\partial \bar{x}_2}{\partial y^2} & \frac{\partial \bar{x}_2}{\partial y^3} \\ \frac{\partial \bar{x}_3}{\partial y^1} & \frac{\partial \bar{x}_3}{\partial y^2} & \frac{\partial \bar{x}_3}{\partial y^3} \end{vmatrix} \quad (94)$$

and the equations are cast into a "semi-strong" conservation form using the following relations,

$$\sum_{j=1}^3 \frac{\partial \hat{y}_{,i}^j}{\partial y^j} = 0 \quad (95)$$

and

$$\frac{\partial J}{\partial \tau} + \sum_{j=1}^3 \frac{\partial \hat{y}_{,t}^j}{\partial y^j} = 0 \quad (96)$$

where

$$\hat{y}_{,i}^j \equiv J y_{,i}^j \quad (97)$$

$$\hat{y}_{,t}^j \equiv J y_{,t}^j$$

The semi-strong conservation form implies that all factors involving the radial coordinate $r = \bar{x}_1$ remain as they were before the Jacobian transformation. The resulting equations are presented in Appendix A.

The geometric relations Eq. (95-96) may be obtained from the transformation relations for $\hat{y}_{,t}^j$ and $\hat{y}_{,i}^j$ in terms of the inverse transformation derivatives (e.g., Ref. 15),

$$\begin{aligned} \hat{y}_{,1}^1 &= \bar{x}_{2,2} \bar{x}_{3,3} - \bar{x}_{2,3} \bar{x}_{3,2} \\ \hat{y}_{,2}^1 &= \bar{x}_{3,2} \bar{x}_{1,3} - \bar{x}_{3,3} \bar{x}_{1,2} \\ \hat{y}_{,3}^1 &= \bar{x}_{1,2} \bar{x}_{2,3} - \bar{x}_{1,3} \bar{x}_{2,2} \\ \hat{y}_{,1}^2 &= \bar{x}_{2,3} \bar{x}_{3,1} - \bar{x}_{2,1} \bar{x}_{3,3} \\ \hat{y}_{,2}^2 &= \bar{x}_{3,3} \bar{x}_{1,1} - \bar{x}_{3,1} \bar{x}_{1,3} \\ \hat{y}_{,3}^2 &= \bar{x}_{1,3} \bar{x}_{2,1} - \bar{x}_{1,1} \bar{x}_{2,3} \\ \hat{y}_{,1}^3 &= \bar{x}_{2,1} \bar{x}_{3,2} - \bar{x}_{2,2} \bar{x}_{3,1} \\ \hat{y}_{,2}^3 &= \bar{x}_{3,1} \bar{x}_{1,2} - \bar{x}_{3,2} \bar{x}_{1,1} \\ \hat{y}_{,3}^3 &= \bar{x}_{1,1} \bar{x}_{2,2} - \bar{x}_{1,2} \bar{x}_{2,1} \end{aligned} \quad (98)$$

and

$$\hat{y}_{,t}^j = - \sum_{k=1}^3 \hat{y}_{,k}^j \frac{\partial \bar{x}_k}{\partial \tau} \quad (99)$$

The projectile motion is assumed to be in the \bar{x}_3 -direction, hence the following normalized nonuniform coordinate, $\eta^3(y^3)$, is introduced:

$$\eta^3(y^3) = \frac{z - z_0}{z_1 - z_0} \quad (100)$$

where z_0 is the Cartesian location of the breech end of the gun barrel and z_1 is the Cartesian location of the first filler element and y^3 is an equally spaced computational coordinate having a value from 1.0 to y^3_{\max} . A similar transformation can be implemented for the radial coordinate, \bar{x}_1 , to permit the tube radius to vary with axial distance, and to allow a concentration of grid points in the \bar{x}_1 -direction as a function of \bar{x}_3 and time t . The latter feature would permit the concentration of \bar{x}_1 -direction grid points in the manner shown in Fig. 2, to account for a variation of the boundary layer thickness as a function of \bar{x}_3 and t as the projectile moves through the barrel. As can be seen in Fig. 2 the resulting coordinate system is nonorthogonal, however, such a system is already encompassed by the general transformation, Eq. (92). Introducing a normalized nonuniform coordinate,

$$\eta^1(y^1) = \frac{r - r_0}{r_1 - r_0} \quad (101)$$

where $r_1 = r_1(\bar{x}_3)$ is the radial location of the tube wall, $r_0 = r_0(\bar{x}_3)$ is the radial location of a centerbody if one exists, and y^1 is an equally spaced computational coordinate having a value from 1.0 to y^1_{\max} . Of course, at the centerline of a tube $r_0 = 0$. The functional forms of $\eta^1(y^1)$ and of $\eta^3(y^3)$ are arbitrary and can be chosen such that the packing of grid points in the \bar{x}_1 or \bar{x}_3 -direction is achieved in the regions where the largest gradients are expected. Presently the computer code allows for the concentration of grid points to occur by means of Levy's (Ref. 38) generalization of the Roberts' transformation (Ref. 39). The grid points can be concentrated at the boundaries of the computational domain or the grid points can be concentrated around some interior location. The transformation equation used for this purpose is

$$\eta^j = \eta^j_0 + \frac{1}{A} \sinh \left\{ C \left[\frac{\tanh(Ey^j + F) - H}{G} \right] + D \right\} \quad (102)$$

where η^j_0 is the value of η^j about which the concentration of grid points is centered and the values of A, C, D, E, F, G and H are controlled by the input parameters, η^j_0 , t_2 , τ_1 and τ_2 . The derivation of the relationships between A, C, D, E, F, G and H and the input parameters is quite lengthy and hence only the results are presented here, viz.,

$$A = \frac{\sinh(t_2)}{\eta^j_{\text{MAX}} - \eta^j_0} \quad (103)$$

$$C = \frac{t_2 - t_1}{y^j_{\text{MAX}} - 1} \quad (104)$$

where

$$t_1 = \ln \left\{ A(\eta^j_{\text{MIN}} - \eta^j_0) + \sqrt{1 + A^2(\eta^j_{\text{MIN}} - \eta^j_0)^2} \right\} \quad (105)$$

and $\eta^j_{\text{min}} = 0$ and $\eta^j_{\text{max}} = 1$.

$$D = t_1 - C \quad (106)$$

$$E = \frac{s_2 - s_1}{y^j_{\text{MAX}} - 1} \quad (107)$$

where

$$s_1 = \frac{\ln \left(\frac{1 + \tau_1}{1 - \tau_1} \right)}{2} \quad (108)$$

$$s_2 = \frac{\ln \left(\frac{1 + \tau_2}{1 - \tau_2} \right)}{2} \quad (109)$$

$$F = s_1 - E \quad (110)$$

$$G = \frac{\tau_2 - \tau_1}{y^j_{\text{MAX}} - 1} \quad (111)$$

$$H = \tau_1 - G \quad (112)$$

The above is presented only for completeness; the important thing to note is the effect that η_0^j , t_2 , τ_1 and τ_2 have on the physical grid spacing. The effect of t_2 is to regulate the sinh portion of the transformation, while τ_1 and τ_2 regulate the tanh portion of the transformation. Note that different parameter values may be specified for each of the coordinate directions \bar{x}_j in order to control the grid spacing in each of those directions; τ_1 controls the physical grid spacing at the lower end (η_{\min}^j) of the computational domain while τ_2 controls the spacing at the upper end (η_{\max}^j). The values of τ_1 and τ_2 are subject to the following limitations

$$\begin{aligned} -1 &< \tau_1 \leq 0 \\ 0 &\leq \tau_2 < 1 \\ t_2 &\geq 0 \end{aligned} \tag{113}$$

In order to see how the input parameters effect the grid spacing it is instructive to first negate the effect of the sinh by setting $t_2 = 0$ and to investigate the effect that τ_1 and τ_2 have on the transformation. If $\tau_1 = 0$ and $\tau_2 > 0$ grid packing will occur at η_{\max}^j (the larger the value of τ_2 the greater the packing) while if $\tau_1 < 0$ and $\tau_2 = 0$ packing occurs at η_{\min}^j (the larger the value of $|\tau_1|$ the greater the packing). Zero values of τ_1 and τ_2 result in equal grid spacing while nonzero values of both τ_1 and τ_2 result in packing at both η_{\min}^j and η_{\max}^j . If $\tau_1 = \tau_2$ and $t_2 = 0$ the transformation Eq. (102) is equivalent to the original transformation of Roberts (Ref. 39), and the parameter τ_2 is related to Roberts' normalized boundary layer thickness parameter σ by $\tau_2 = (1-\sigma)^{1/2}$. On the other hand if the effect of the tanh is negated by setting both τ_1 and τ_2 equal to zero, the effect is to concentrate the grid points about η_0^α only. The larger the value of t_2 the greater the concentration. Nonzero values of t_2 , τ_1 and τ_2 result in a combination of the effects of the sinh and the tanh transformations.

SOLUTION PROCEDURE

The development of the ALPHA2 computer code is based upon an axisymmetric version of the highly efficient consistently split, linearized block-implicit solution procedure (MINT) for the compressible Navier-Stokes equations developed by Briley and McDonald (Ref. 16-18), and subsequently extended to multi-component, chemically reacting, turbulent flows by Gibeling, McDonald and Briley (Ref. 19). This procedure solves the Navier-Stokes equations written in primitive variables; in the MINT procedure, the governing equations are replaced by either a Crank-Nicholson or a backward time difference approximation. Terms involving nonlinearities at the implicit time level are linearized by Taylor series expansion about the known time level, and spatial difference approximations are introduced. The result is a system of two-dimensional coupled linear difference equations for the dependent variables at the unknown or implicit time level. These equations are solved by the Douglas-Gunn (Ref. 40) procedure for generating ADI schemes as perturbations to fundamental implicit difference schemes. This technique leads to systems of one-dimensional coupled linear difference equations which are solved by standard block-elimination methods, with no iteration required to compute the solution for a given time step. An artificial dissipation term based upon either a cell Reynolds number criterion or the rate of change of the dependent variable may be introduced selectively into the scheme to allow calculations to be performed at high local values of the cell Reynolds number.

The use of an implicit solution procedure requires that equation coupling and linearization be considered. Both of these questions are reviewed in detail by McDonald and Briley (Ref. 41) and Briley and McDonald (Ref. 18). These authors have argued that for a given grid the errors arising from time linearization of the nonlinear terms at the unknown time level should be no greater than the discretization errors. Also, reduction of the time step is the preferred way of reducing the linearization error since transient accuracy is thereby improved. Linearization by Taylor series expansion in time about the known time level introduces errors no greater than those due to the differencing (Refs. 41 and 18), and this approach has been employed in the ALPHA2 code. The formal linearization process results in a system of coupled equations in order to retain second-order temporal accuracy. The system of coupled equations at the implicit time level is solved efficiently using a standard block elimination matrix inversion scheme. In the present problem, the strong coupling effects among the governing equations dictate the use of the

block coupled equation approach. However, weakly coupled equations would probably be solved in a decoupled manner in order to reduce computer time and storage requirements.

The principal partial differential equations which will be solved via the MINT technique are: gas and solid phase continuity, gas and solid phase momenta, gas phase energy, gas phase turbulence kinetic energy, gas phase mixture molecular weight and specific heat equations and the particle radius equation. The constitutive relations required to close the above system of equations have been specified above. The solid phase heat conduction equation is the only differential equation which requires special treatment because it is a Lagrangian equation.

The scheme devised for solution of the solid phase heat conduction equation is unique since it does not involve the use of marker particles introduced by other authors (e.g., Ref. 2). This is possible because the equation is a simple heat conduction equation for a representative solid particle moving at a velocity \vec{U}_p which is known at the completion of a given time step. The necessary boundary conditions, Eqs. (35-38), provide information about the environment through which the particle is moving in the form of a heat transfer coefficient, Eq. (39). The procedure to be used assumes that at time t^{n+1} the representative particle has moved to the grid point $\vec{x}_{i,j,k}^{n+1} = (x_1^{n+1}, x_2^{n+1}, x_3^{n+1})$ from a location at time t^n which is determined from the known absolute particle velocities \vec{v}_p^{n+1} and \vec{v}_p^n , i.e., if \vec{s}_p is the particle position vector relative to an inertial reference frame, we have

$$\frac{d\vec{s}_p}{dt} = \vec{v}_p \quad (114)$$

and application of the variable time differencing scheme yields,

$$\vec{s}_p^{n+1} = \vec{s}_p^n + [\beta \vec{v}_p^{n+1} + (1-\beta) \vec{v}_p^n] \Delta t \quad (115)$$

where $\beta = 1$ for backward time differencing and $\beta = 1/2$ for Crank-Nicholson (centered) time differencing. In the present scheme, \vec{s}_p^{n+1} is assumed to be the grid point location $\vec{x}_{i,j,k}^{n+1}$ and Eq. (115) is then solved for \vec{s}_p^n . Because the grid is moving it is necessary to interpolate to find the required value of the particle velocity at time t^n at space point $\vec{x}_{i,j,k}^{n+1}$, $\vec{v}_p^n = \vec{v}_p^n(\vec{x}_{i,j,k}^{n+1}, t^n)$. The boundary condition, Eq. (38), may then be written as

$$\begin{aligned}
 \frac{k_p}{r_p} \frac{\partial \bar{T}_p}{\partial \zeta} (\zeta = 1, t^{n+1}) &= \beta \left[h_f(t^{n+1})(\bar{T}^{n+1} - \bar{T}_{ps}^{n+1}) + k_p \phi(R_s^{n+1}, p^{n+1}) \right] \\
 &+ (1 - \beta) \left[h_f(t^n)(\bar{T}^n - \bar{T}_{ps}^n) + k_p \phi(R_s^n, p^n) \right] \quad (116)
 \end{aligned}$$

The desired properties $h_f(t^n)$, \bar{T}^n , \bar{T}_{ps}^n , and $\phi(R_s^n, p^n)$ are understood to be evaluated at the point \vec{s}_p^n , and these will be evaluated by interpolation utilizing values at time t^n at the four grid points surrounding point \vec{s}_p^n .

Finally, the governing equation (32) and boundary conditions, Eq. (35) and (116), may be written in finite difference form. The resulting tridiagonal matrix is easily inverted using Gaussian elimination to yield the temperature distribution within the particle. Another approximate solution technique could be incorporated at a later time in order to reduce the computer requirements for the particle heat conduction model.

Initial and Boundary Conditions

The initial conditions for the first phase of two-dimensional calculations will consist of a description of the fluidized state of the flow in a gun barrel after ignition is complete and the projectile motion has begun. Typically, the necessary data would be produced from an existing one-dimensional interior ballistics computer code, and would then be extended over the two-dimensional computational domain by applying a correction for the wall boundary layers. Provisionally, the boundary layer integral method adopted by Gough (Ref. 2) would be utilized to determine the boundary layer thickness and velocity profile.

The boundary conditions to be applied would be no-slip gas velocities on solid surfaces and conventional symmetry conditions at the tube centerline. The breech would be assumed to be stationary, and, of course, the projectile and filler elements would be allowed to move. The wall pressure would be determined by employing the normal gas momentum equation written at the wall. The surface temperature would be determined by incorporating a barrel heat conduction model coupled to the gas heat transfer at the wall. For simplicity, heat conduction in the barrel would be assumed to be primarily in the radial direction. The porosity at a wall would be determined from either the solid phase continuity equation, Eq. (8), or a zero normal derivative condition. The solid phase velocities at a wall would be determined from either the no-slip condition or the solid phase momentum equations written at the wall.

The appropriate boundary condition for the inverse mixture molecular weight (Z), specific heat (c_p), and particle radius (r_p) at a solid wall is zero normal derivative, i.e.,

$$\left(\frac{\partial Z}{\partial n} \right)_w = \left(\frac{\partial c_p}{\partial n} \right)_w = \left(\frac{\partial r_p}{\partial n} \right)_w = 0 \quad (117)$$

This follows from the definition of these quantities as mass weighted averages, and the assumption that the individual species diffusion velocities normal to the wall as determined from Fick's law must be zero; that is, $(\partial m_j / \partial n) = 0$ where m_j is a species mass fraction.

The solid particles which reach the wall will be assumed to be in equilibrium with the gas phase, thus

$$(\bar{T}_{ps})_w = (\bar{T})_w \quad (118)$$

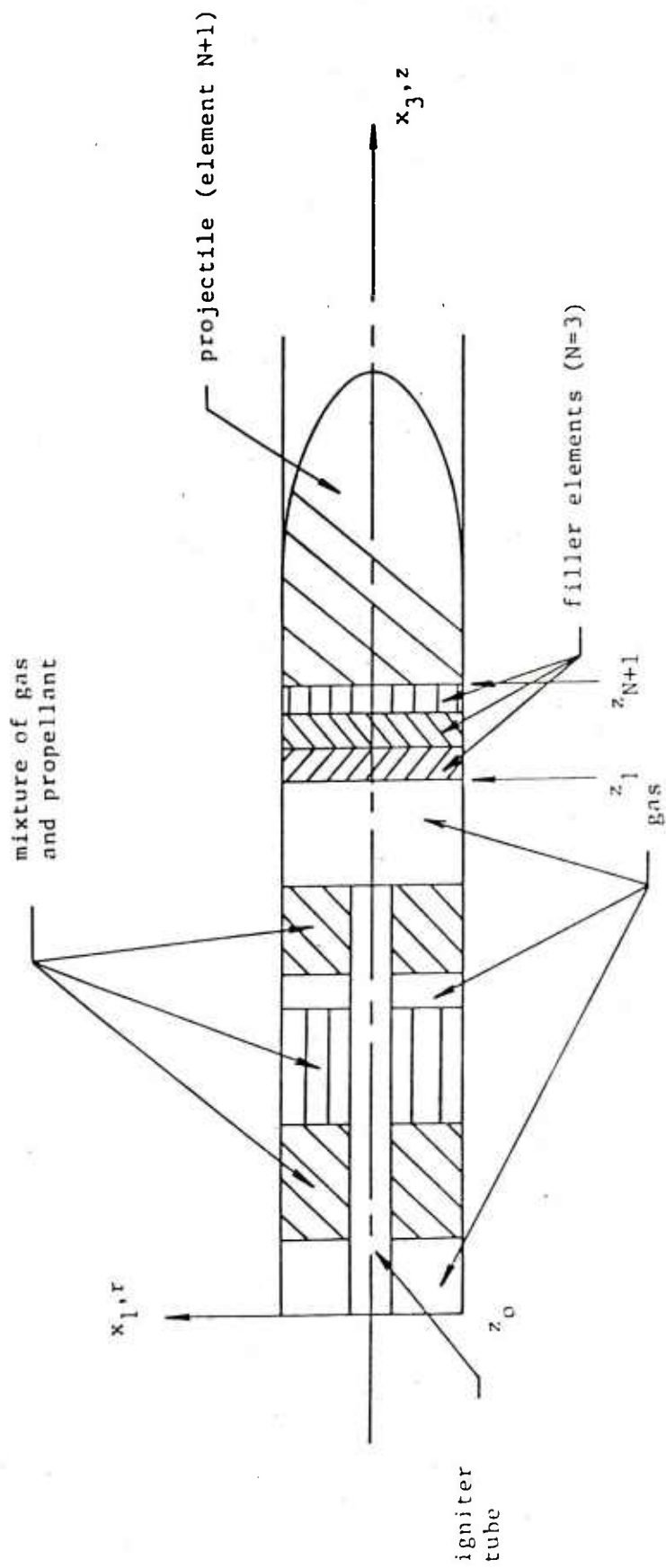


Figure 1. Schematic illustration of gun breech region prior to firing

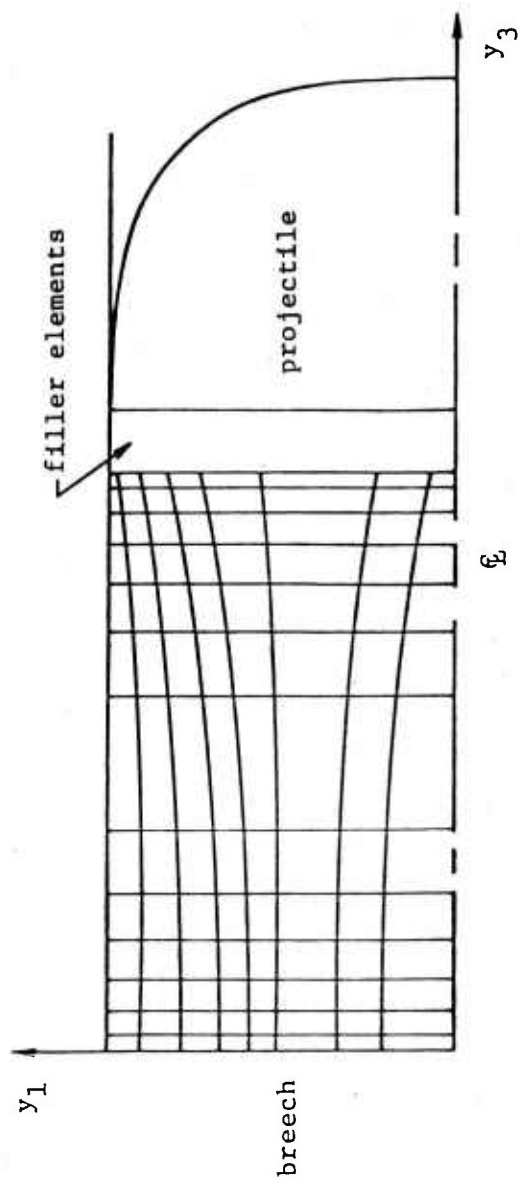


Figure 2. Mesh distribution scheme

References

1. Gibeling, H. J., Buggeln, R. C., and McDonald, H.: Development of a Two-Dimensional Implicit Interior Ballistics Code, U. S. Army Armament Research and Development Command, Ballistic Research Laboratory Report ARBRL-CR-00411, January 1980. (AD #A084092)
2. Gough, P. S.: Numerical Analysis of a Two-Phase Flow with Explicit Internal Boundaries. IHCR 77-5, Naval Ordnance Station, Indian Head, MD, April 1977.
3. Koo, J. H., and Kuo, K. K.: Transient Combustion in Granular Propellant Beds. Part 1: Theoretical Modeling and Numerical Solution of Transient Combustion Processes in Mobile Granular Propellant Beds. BRL CR-346, U. S. Army Ballistic Research Laboratory, Aberdeen Proving Ground, MD, August 1977. (AD #A044998).
4. Kuo, K. K., Koo, J. H., Davis, T. R., and Coates, G. R.: Transient Combustion in Mobile Gas-Permeable Propellants. Acta Astronautica, Vol. 3, 1976, pp. 573-591.
5. Fisher, E. B., Graves, K. W., and Trippe, A. P.: Application of a Flame Spread Model to Design Problems in the 155 mm Propelling Charge. 12th JANNAF Combustion Meeting, CPIA Publication 273, Vol. I, December 1975, p. 199.
6. Krier, H., Rajan, S., and Van Tassell, W.: Flame Spreading and Combustion in Packed Beds of Propellant Grains. AIAA Journal, Vol. 14, No. 3, March 1976, p. 301.
7. Krier, H., and Gokhale, S. S.: Modeling of Convective Mode Combustion Through Granulated Propellant to Predict Detonation Transition. AIAA J., Vol. 16, No. 2, 1978, pp. 177-183.
8. Gough, P. S.: Two-Dimensional Convective Flamespreading in Packed Beds of Granular Propellant, U. S. Army Armament Research and Development Command, Ballistic Research Laboratory Report ARBRL-CR-00404, July 1979. (AD #A075326)
9. Anderson, L. W., Bartlett, E. P., Dahm, T. J., and Kendall, R. M.: Numerical Solution of the Nonsteady Boundary Layer Equations with Application to Convective Heat Transfer in Guns. Aerotherm Report No. 70-22, Aerotherm Corp., October 1970.
10. Bartlett, E. P., Anderson, L. W., and Kendall, R. M.: Time-Dependent Boundary Layers with Application to Gun Barrel Heat Transfer. Proceedings 12th Heat Transfer and Fluid Mechanics Institute, Stanford Univ. Press, 1972, p. 262.
11. Kuo, K. K.: A Summary of the JANNAF Workshop on "Theoretical Modeling and Experimental Measurements of the Combustion and Fluid Flow Processes in Gun Propellant Charges". 13th JANNAF Combustion Meeting, CPIA Publication 281, Vol. I, December 1976, p. 213.
12. MacCormack, R. W.: The Effect of Viscosity in Hypervelocity Impact Cratering, AIAA Paper No. 69-354, 1969.

References (Continued)

13. Moretti, G.: Calculation of the Three-Dimensional Supersonic, Inviscid, Steady Flow Past an Arrow-Winged Airframe, POLY-AE/AM Report No. 76-8, 1976.
14. Thompson, J. F., Thames, F. C., and Mastin, C. W.: Automatic Numerical Generation of Body-Fitted Circular Coordinate System for Field Containing Any Number of Arbitrary Two-Dimensional Bodies, *J. Comp. Physics*, Vol. 15, 1974, p. 299.
15. Thames, P. D., and Lombard, C. K.: Geometric Conservation Law and Its Application to Flow Computations on Moving Grids, *AIAA Journal*, Vol. 17, No. 10, 1979, p. 1030.
16. Briley, W. R., and McDonald, H.: An Implicit Numerical Method for the Multi-dimensional Compressible Navier-Stokes Equations. United Aircraft Research Laboratories Report M911363-6, November 1973.
17. Briley, W. R., McDonald, H., and Gibeling, H. J.: Solution of the Multi-dimensional Compressible Navier-Stokes Equations by a Generalized Implicit Method. United Technologies Research Center Report R75-911363-15, January 1976.
18. Briley, W. R., and McDonald, H.: Solution of the Multidimensional Compressible Navier-Stokes Equations by a Generalized Implicit Method. *J. Comp. Physics*, Vol. 24, No. 4, 1977, p. 372.
19. Gibeling, H. J., McDonald, H., and Briley, W. R.: Development of a Three-Dimensional Combustor Flow Analysis. AFAPL-TR-75-59, Vol. I, July 1975 and Volume II, October 1976.
20. Briley, W. R., and McDonald, H.: On the Structure and Use of Linearized Block ADI and Related Schemes. *J. Comp. Physics*, Vol. 34, No. 1, 1980, p. 54.
21. Ishii, M.: Thermo-Fluid Dynamic Theory of Two-Phase Flow. Eyrolles, Paris, 1975.
22. Gough, P. S.: Derivation of Balance Equations for Heterogeneous Two-Phase Flow by Formal Averaging. ARO Workshop on Multiphase Flows, Ballistic Research Laboratory, February 1978, pp. 71-80.
23. Gough, P. S.: The Flow of a Compressible Gas Through an Aggregate of Mobile, Reacting Particles. Ph.D Thesis, Department of Mechanical Engineering, McGill University, Montreal, 1974.
24. Gough, P. S. and Zwarts, F. J.: Some Fundamental Aspects of the Digital Simulation of Convective Burning in Porous Beds. AIAA Paper 77-855, July 1977.
25. Bradshaw, P. and Ferriss, D. H.: Calculation of Boundary-Layer Development Using the Turbulent Energy Equation: Compressible Flow on Adiabatic Walls. *J. Fluid Mechanics*, Vol. 46, Part 1, 1971, pp. 83-110.

References (Continued)

26. Launder, B. E., and Spalding, D. B.: The Numerical Computation of Turbulent Flows. Computer Methods in Applied Mechanics and Engineering, Vol. 3, 1974, p. 269.
27. Jones, W. P., and Launder, B. E.: The Prediction of Laminarization with a Two-Equation Model of Turbulence. Int. J. Heat Mass Transfer, Vol. 15, 1972, p. 301.
28. Shamroth, S. J., and Gibeling, H. J.: A Compressible Solution of the Navier-Stokes Equations for Turbulent Flow About an Airfoil, NASA CR-3183, 1979.
29. McDonald, H., and Fish, R. W.: Practical Calculation of Transitional Boundary Layers. Int. J. Heat and Mass Transfer, Vol. 16, No. 9, 1973, pp. 1729-1744.
30. Shamroth, S. J., and McDonald, H.: Assessment of a Transitional Boundary Layer Theory at Low Hypersonic Mach Numbers. Int. J. Heat and Mass Transfer, Vol. 18, 1975, pp. 1277-1284.
31. Kreskovsky, J. P., Shamroth, S. J., and McDonald, H.: Application of a General Boundary Layer Analysis to Turbulent Boundary Layers Subjected to Strong Favorable Pressure Gradients. J. Fluid Eng., Vol. 97, June 1975, pp. 217-224.
32. Williamson, J. W.: An Extension of Prandtl's Mixing Length Theory. Applied Mechanics and Fluids Engineering Conference, ASME, June 1969.
33. Van Driest, E. R.: On Turbulent Flow Near a Wall. Journal of the Aeronautical Sciences, November 1956.
34. Ergun, S.: Fluid Flow Through Packed Columns. Chem. Eng. Progr., Vol. 48, 1952, p. 89.
35. Anderssen, K. E. B.: Pressure Drop in Ideal Fluidization. Chemical Engineering Science, Vol. 15, 1961, pp. 276-297.
36. Gelperin, N. I. and Einstein, V. G.: Heat Transfer in Fluidized Beds. In Fluidization, edited by J. F. Davidson and D. Harrison, Academic Press, 1971.
37. Lenoir, J. M. and Robillard, G.: A Mathematical Method to Predict the Effects of Erosive Burning in Solid-Propellant Rockets. Sixth Symposium (International) on Combustion, Combustion Institute, 1957, pp. 663-667.
38. Levy, R., and Gibeling, H. J.: Coordinate Transformations for Grid Point Packing, SRA Report R80-2, 1980.
39. Roberts, G. E.: Computational Meshes for Boundary Layer Problems. Proceedings of the Second International Conference on Numerical Methods in Fluid Dynamics, Springer-Verlag, New York, 1971, p. 171.
40. Douglas, J., and Gunn, J. E.: A General Formulation of Alternating Direction Methods. Numerische Math., Vol. 6, 1964, p. 428.
41. McDonald, H., and Briley, W. R.: Three-Dimensional Flow of a Viscous or Inviscid Gas. J. Comp. Physics, Vol. 19, No. 2, 1975, p. 150.

APPENDIX

The governing conservation equations in cylindrical-polar coordinates are transformed using the Jacobian transformation,

$$y^j = y^j(\bar{x}_1, \bar{x}_2, \bar{x}_3, t) \quad (A-1)$$

$$\tau = t$$

where $(\bar{x}_1, \bar{x}_2, \bar{x}_3) = (r, \theta, z)$. The resulting equations may be written in the following compact form:

$$\begin{aligned} \frac{\partial(J\bar{W})}{\partial\tau} = & - \sum_{j=1}^3 \left\{ \frac{\partial}{\partial y^j} (J y^j \bar{W}) + \sum_{i=1}^3 \left[\beta_i \frac{\partial}{\partial y^j} (J y^j_i \bar{F}_i) \right. \right. \\ & \left. \left. + \tilde{\alpha} \gamma_i \frac{\partial}{\partial y^j} (J y^j_i \bar{P}_i) - \zeta_i \frac{\partial}{\partial y^j} (J y^j_i \bar{G}_i) \right] \right\} \\ & + J\bar{S} + J\bar{C} \end{aligned} \quad (A-2)$$

where

$$\begin{aligned} y^j_t & \equiv \frac{\partial y^j}{\partial t} \\ y^j_i & \equiv \frac{\partial y^j}{\partial \bar{x}_i} \end{aligned} \quad (A-3)$$

Further, the coefficients β_i , γ_i , ζ_i are given by

$$\begin{aligned} \beta_1 & = \frac{1}{r} , \quad \beta_2 = \frac{1}{r} , \quad \beta_3 = 1 \\ \gamma_1 & = 1 , \quad \gamma_2 = \frac{1}{r} , \quad \gamma_3 = 1 \\ \zeta_1 & = \frac{1}{r^m} , \quad \zeta_2 = \frac{1}{r} , \quad \zeta_3 = 1 \end{aligned} \quad (A-4)$$

and $m = 1$ for all equations except the \bar{x}_2 -direction momentum equations (gas and solid phase), for which $m = 2$. The quantity α is

$$\begin{aligned} \tilde{\alpha} & = \alpha \quad \text{for gas phase equations} \\ \tilde{\alpha} & = 1 - \alpha \quad \text{for solid phase equations} \end{aligned} \quad (A-5)$$

The vector variables used in Eq. (A-2) are defined as

$$\vec{w} = \begin{bmatrix} \alpha \rho U_1 \\ \alpha \rho U_2 \\ \alpha \rho U_3 \\ \alpha \rho \\ \alpha \rho h \\ \alpha \rho k \\ \alpha \rho c_p \\ \alpha \rho z \\ (1-\alpha) \rho_p r_p \\ (1-\alpha) \rho_p U_{p1} \\ (1-\alpha) \rho_p U_{p2} \\ (1-\alpha) \rho_p U_{p3} \\ (1-\alpha) \rho_p \end{bmatrix} \quad (A-6)$$

$$\vec{F}_i = r^n \begin{bmatrix} \alpha \rho U_i U_i \\ \alpha \rho U_2 U_i \\ \alpha \rho U_3 U_i \\ \alpha \rho U_i \\ \alpha \rho h U_i \\ \alpha \rho k U_i \\ \alpha \rho c_p U_i \\ \alpha \rho z U_i \\ (1-\alpha) \rho_p r_p U_{pi} \\ (1-\alpha) \rho_p U_{p1} U_{pi} \\ (1-\alpha) \rho_p U_{p2} U_{pi} \\ (1-\alpha) \rho_p U_{p3} U_{pi} \\ (1-\alpha) \rho_p U_{pi} \end{bmatrix} \quad (A-7)$$

where $n = 1$ for $i = 1$ and $n = 0$ for $i = 2, 3$.

$$\vec{P}_i = \begin{bmatrix} p \delta_{i1} \\ p \delta_{i2} \\ p \delta_{i3} \\ 0 \\ 0 \\ 0 \\ 0 \\ 0 \\ p \delta_{i1} \\ p \delta_{i2} \\ p \delta_{i3} \\ 0 \end{bmatrix} \quad (A-8)$$

$$\vec{G}_i = \begin{bmatrix} \alpha r \tau_{11} \\ \alpha r^2 \tau_{12} \\ \alpha r \tau_{13} \\ 0 \\ -\alpha r q_1 \\ \alpha \frac{\mu_T}{\sigma_k} \gamma_1 k_{,1} \\ \alpha \Gamma_m \gamma_1 c_{p,1} \\ \alpha \Gamma_m \gamma_1 z_{,1} \\ (1-\alpha) \Gamma_m \gamma_1 r_{p,1} \\ (1-\alpha) r R_{11} \\ (1-\alpha) r^2 R_{12} \\ (1-\alpha) r R_{13} \\ 0 \end{bmatrix} \quad (A-9)$$

$$\vec{G}_i = \begin{bmatrix} a\tau_{i1} \\ a\tau_{i2} \\ a\tau_{i3} \\ 0 \\ -a\dot{q}_i \\ a\frac{\mu_T}{\sigma_k} \gamma_i k_{,i} \\ a\Gamma_m \gamma_i c_{p,i} \\ a\Gamma_m \gamma_i z_{,i} \\ (1-a)\Gamma_m \gamma_i r_{p,i} \\ (1-a)R_{i1} \\ (1-a)R_{i2} \\ (1-a)R_{i3} \\ 0 \end{bmatrix} \quad \text{for } i=2,3 \quad (A-10)$$

Note that the velocity components (U_1, U_2, U_3) and (U_{p1}, U_{p2}, U_{p3}) are the cylindrical-polar velocity components, and τ_{ij} and R_{ij} are the gas-phase stress tensor and the solid phase intergranular stress tensor, respectively, written in cylindrical-polar coordinates. The molecular and turbulent stress tensors, Eqs. (19) and (22), may be written as

$$\tau_{ij} = 2\mu_{eff} \bar{D}_{ij} - \frac{2}{3} \mu_{eff} (\nabla \cdot \vec{U}) \delta_{ij} + \frac{2}{3} (K_B \nabla \cdot \vec{U} - \rho k) \delta_{ij} \quad (A-11)$$

and the rate of strain tensor components in cylindrical-polar coordinates are

$$\begin{aligned} \bar{D}_{11} &= \frac{\partial U_1}{\partial \bar{x}_1} \\ \bar{D}_{22} &= \frac{1}{r} \frac{\partial U_2}{\partial \bar{x}_2} + \frac{U_1}{r} \\ \bar{D}_{33} &= \frac{\partial U_3}{\partial \bar{x}_3} \\ \bar{D}_{12} &= \frac{1}{2} \left[r \frac{\partial}{\partial \bar{x}_1} \left(\frac{U_2}{r} \right) + \frac{1}{r} \frac{\partial U_1}{\partial \bar{x}_2} \right] \\ \bar{D}_{13} &= \frac{1}{2} \left[\frac{\partial U_3}{\partial \bar{x}_1} + \frac{\partial U_1}{\partial \bar{x}_3} \right] \\ \bar{D}_{23} &= \frac{1}{2} \left[\frac{1}{r} \frac{\partial U_3}{\partial \bar{x}_2} + \frac{\partial U_2}{\partial \bar{x}_3} \right] \end{aligned} \quad (A-12)$$

and

$$\nabla \cdot \vec{U} = \frac{1}{r} \frac{\partial}{\partial \bar{x}_1} (r U_1) + \frac{1}{r} \frac{\partial U_2}{\partial \bar{x}_2} + \frac{\partial U_3}{\partial \bar{x}_3} \quad (A-13)$$

Also, an isotropic intergranular stress tensor is assumed,

$$R_{ij} = R_p \delta_{ij} \quad (A-14)$$

where the constitutive relation for R is given by Eq. (70). Therefore, the intergranular stress becomes a normal stress as is the gas pressure. The derivatives required in Eqs. (A-12, A-13) must be expressed in terms of the computational coordinates y^j using the chain rule, Eq. (92).

Finally, the vector \vec{S} contains source terms and certain differential terms which do not conform to the basic structure of Eq. (A-2), and the vector \vec{C} contains the additional curvature terms due to the cylindrical-polar coordinate system.

$$\vec{S} = \begin{bmatrix} M_1 \\ M_2 \\ M_3 \\ \Gamma \\ \Lambda + \frac{D(\alpha_p)}{Dt} + \alpha \Phi + \alpha \rho \epsilon \\ \alpha \left\{ \mu_T \left[2 \bar{D}_{ij} \bar{D}_{ij} - \frac{2}{3} (\nabla \cdot \vec{U})^2 \right] - \frac{2}{3} \rho k \nabla \cdot \vec{U} - \rho \epsilon \right\} + S_k \\ (C_p)_p \Gamma \\ z_p \Gamma \\ - (1 - \alpha) \rho_p \left(1 + r_p \frac{S_p}{V_p} \right) \langle \dot{d} \rangle^i \\ - M_1 \\ - M_2 \\ - M_3 \\ - \Gamma \end{bmatrix} \quad (A-15)$$

where

$$\vec{M} = -(1-\alpha) \frac{S_p}{V_p} \langle \vec{F} \rangle^i + \vec{U}_p \Gamma \quad (A-17)$$

The quantities Γ , $\langle \vec{F} \rangle^i$, $\langle \vec{d} \rangle^i$, and Λ are defined in Eqs. (18), (71), (79) and (29), respectively.

LIST OF SYMBOLS

a_p	reference speed of sound in solid phase
A	transformation parameter, Eq. (103)
A_i	local area of filler element i
c_p	specific heat at constant pressure
c_v	specific heat at constant pressure
C	transformation parameter, Eq. (104)
C_μ	constant in turbulent viscosity relation, Eq. (49)
\dot{d}	instantaneous surface regression rate
\dot{d}_E	average surface regression rate for erosive burning, Eq. (80)
\dot{d}_s	average steady state surface regression rate, Eq. (79)
$\langle \dot{d} \rangle^i$	average regression rate of solid phase
D	transformation parameter, Eq. (106)
D_B	diameter of launching tube
\mathbb{D}	total deformation tensor, Eq. (20)
\mathbb{D}_b	bulk deformation tensor, Eq. (21)
\mathbb{D}_i	interfacial deformation tensor
e	internal energy per unit mass
E	transformation parameter, Eq. (107)
F	transformation parameter, Eq. (110)
F_i	resistance force opposing motion of filler element i
F_{wi}	normal wall reaction force on filler element i , Eq. (85)
$\langle \dot{F} \rangle$	interphase drag per unit area of solid phase, Eq. (71)
g	general weighting function for phase averaging, Eqs. (1-3)
G	transformation parameter, Eq. (111)
h	static enthalpy
h_c	convective heat transfer coefficient, Eq. (77)
h_{ig}	enthalpy of igniter gas
h_t	total heat transfer coefficient, Eq. (39)
H	transformation parameter, Eq. (112)
I	projectile polar moment of inertia
\mathbb{I}	identity tensor
J	Jacobian determinant of inverse coordinate transformation, Eq. (94)
\bar{k}	turbulence kinetic energy (gas phase)

k_p	thermal conductivity of solid particles
K_B	bulk viscosity coefficient
K_E	erosive burning constant, Eq. (80)
ℓ	characteristic length scale for turbulent motion (dissipation length scale)
L_D	dimensional reference length
M_i	mass of filler element i , Eqs. (81-84)
\dot{M}	gas-solid momentum exchange, Eq. (A-17)
M_{ig}	rate of mass addition of igniter gas
\vec{n}	outward normal from the gas phase
N	total number of filler elements excluding projectile
Nu_p	Nusselt number for interphase heat transfer correlation Eq. (76)
p	pressure
Pr	Prandtl number, $Pr = \mu c_p / \kappa$
Pr_{eff}	effective Prandtl number for turbulent flow
\vec{q}	heat flux vector
q_{rad}	net incident radiation heat flux normal to solid particle surface, Eq. (37)
$\langle q \rangle^i$	interphase heat transfer relation, Eq. (78)
\tilde{r}	radial coordinate within a spherical solid particle
r_p	average radius of a spherical solid particle; $r_p(x, t)$
\mathbb{R}	granular stress tensor, solid phase, Eq. (23)
Re_p	Reynolds number based upon gas density particle diameter and relative velocity, Eq. (75)
R_p	isotropic normal stress in the solid phase, Eq. (70)
R_s	average surface regression rate, Eq. (33)
R_u	universal gas constant
\vec{s}_p	position vector of solid particle, Eq. (115)
s_1	defined by Eq. (100)
s_2	defined by Eq. (109)
S_1	constant in Sutherland's law, Eq. (46)
S_2	constant in thermal conductivity relation, Eq. (48)
S_k	production of turbulence kinetic energy due to inter- action between gas and solid phases, Eq. (68)
S_p	average particle surface area
t	time
t_1	defined by Eq. (105)

t_2	grid concentration parameter associated with sinh transformation
$\bar{\bar{T}}_i$	mean temperature at the interface between the phases (film temperature)
$\bar{\bar{T}}_p$	phase-averaged temperature in solid particle, Eq. (30)
$\bar{\bar{T}}_{ps}$	solid particle temperature
$\bar{\bar{T}}_{po}$	initial particle temperature
T_o	reference temperature in Sutherland's law, Eq. (46)
\vec{u}	instantaneous gas velocity
\vec{u}^i	velocity of the interface between the phases
\vec{u}_p	instantaneous solid phase velocity
\vec{U}	Favré-averaged velocity vector
\vec{U}_{ig}	velocity of igniter gas
\vec{U}_R	relative velocity between gas and solid phases, $\vec{U}_R = \vec{U} - \vec{U}_p$
U_1	\vec{x}_1 -direction velocity component
U_2	\vec{x}_2 -direction velocity component
U_3	\vec{x}_3 -direction velocity component
\vec{v}_p	absolute solid particle velocity vector
V	volume
V_{gas}	volume occupied by gas phase
V_p	average particle volume
W_m	gas phase mixture molecular weight
$\vec{x}_1, \vec{x}_2, \vec{x}_3$	cylindrical polar coordinates, (r, θ, z)
\vec{x}	Cartesian position vector
y^j	computational coordinate
z_i	axial position of left-hand boundary of filler element i , (Fig. 1)
\dot{z}_i	velocity of left-hand boundary of filler element i , (Eqs. (86-87))
\ddot{z}_i	acceleration of left-hand boundary of filler element i , (Eqs. (81-83))
Z	inverse of gas phase mixture molecular weight
α	porosity
α_c	critical or settling porosity above which there is no direct contact between solid particles
α_p	thermal diffusivity of solid particles [$\alpha_p = \kappa_p / \rho_p (c_p)_p$]

β	time differencing parameter, $0.5 \leq \beta \leq 1.0$
β_E	erosive burning constant in Eq. (80)
Γ_1	mass source due to propellant burning
$\bar{\epsilon}$	dissipation rate of turbulence kinetic energy
ϵ_p	emissivity of solid particles
ζ	transformed radial coordinate within a spherical solid particle, Eq. (31)
η	covolume factor in Noble-Abel equation of state, Eq. (41).
η_j	transformed normalized coordinate, Eq. (102)
η_o	value of transformed coordinate η at concentration center, see Eq. (102).
Λ	gas-solid energy exchange rate per unit volume, Eq. (29)
θ	angle of rifling in launching tube
κ	gas phase thermal conductivity, Eq. (48)
κ_p	thermal conductivity of solid particles
μ	molecular viscosity coefficient, Eq. (46)
μ_{eff}	effective viscosity, Eq. (56)
μ_T	turbulent viscosity, Eq. (49)
μ_0	reference molecular viscosity at temperature T_0 in Sutherland's law, Eq. (46)
π	stress tensor, gas phase, Eq. (19)
π^T	turbulent stress tensor (Reynolds stress), Eq. (22)
ρ	density
ρ_k	density of the k^{th} -phase
$\bar{\rho}_m$	mixture density
σ	Stefan-Boltzmann constant
σ_i	internal stress in filler element i , Eq. (86)
σ_k	constant appearing in turbulence kinetic energy equation, Eq. (12)
Σ	region of integration defined by interphase surface and time
τ_1	grid concentration parameter, Eqs. (108-113)
τ_2	grid concentration parameter, Eq. (108-113)
ϕ	heat feedback due to solid particle combustion, Eq. (40); general variable.
Φ	mean flow dissipation function, Eq. (28)

ψ general property of gas or solid phase
 ψ_k property of the k^{th} phase

Superscripts

F Favré-averaged quantity
 T Turbulent quantity
 $(\bar{})$ unnormalized averaged quantity, Eq. (3)
 $(\bar{\bar}{})$ phase-averaged quantity, Eq. (3)
 $(\cdot)'$ fluctuating component
 $(\cdot)^n$ quantity at time t^n

Subscripts

D dimensional reference quantity
 max maximum
 min minimum
 p solid phase property
 ps particle surface value
 T turbulent quantity
 w wall value
 1 associated with first coordinate direction
 2 associated with second coordinate direction
 3 associated with third coordinate direction

DISTRIBUTION LIST

<u>No. of Copies</u>	<u>Organization</u>	<u>No. of Copies</u>	<u>Organization</u>
12	Commander Defense Technical Info Center ATTN: DDC-DDA Cameron Station Alexandria, VA 22314	5	Commander US Army Armament Research and Development Command ATTN: DRDAR-LCU-EP, S. Einstein S. Bernstein DRDAR-LCU-S, R. Corn DRDAR-TDS, V. Lindner DRDAR-TD, E. Friedman Dover, NJ 07801
2	HQDA(DAMA-CSM-CS, LTC Townsend, COL Zimmerman) Washington, DC 20310		
1	Commander US Army Materiel Development and Readiness Command ATTN: DRCDMD-ST 5001 Eisenhower Avenue Alexandria, VA 22333	1	Commander US Army Armament Materiel Readiness Command ATTN: DRSAR-LEP-L, Tech Lib Rock Island, IL 61299
3	Commander US Army Armament Research and Development Command ATTN: DRDAR-CG, MG Lewis Dover, NJ 07801	2	Commander US Army Armament Research and Development Command Benet Weapons Laboratory, LCWSL ATTN: A. Hussain DRDAR-LCB-TL Watervliet Arsenal, NY 12189
6	Commander US Army Armament Research and Development Command ATTN: DRDAR-TSS (2 cys) DRDAR-LC, COL Kenyon DRDAR-LCA, H. Fair D. Down G. Bubb Dover, NJ 07801	1	Commander US Army Aviation Research and Development Command ATTN: DRSAV-E P.O. Box 209 St. Louis, MO 63166
6	Commander US Army Armament Research and Development Command ATTN: DRDAR-LCU, A. Moss D. Costa R. Reisman E. Wurzel DRDAR-LCU-E, S. Westley D. Katz Dover, NJ 07801	1	Director US Army Air Mobility Research and Development Laboratory Ames Research Center Moffett Field, CA 94035
		1	Commander US Army Communications Research and Development Command ATTN: DRDCO-PPA-SA Fort Monmouth, NJ 07703

DISTRIBUTION LIST

<u>No. of Copies</u>	<u>Organization</u>	<u>No. of Copies</u>	<u>Organization</u>
1	Commander US Army Electronics Research and Development Command Technical Support Activity ATTN: DELSD-L Fort Monmouth, NJ 07801	2	Commander US Army Research Office ATTN: J. Chandra E. Singleton P.O. Box 12211 Research Triangle Park, NC 27709
1	Commander US Army Missile Research and Development Command ATTN: DRSMI-R Redstone Arsenal, AL 35809	1	Director US Army TRADOC Systems Analysis Activity ATTN: ATAA-SL, Tech Lib White Sands Missile Range, NM 88002
1	Commander US Army Missile Research and Development Command ATTN: DRSMI-YDL Redstone Arsenal, AL 35809	1	Commander US Army Field Artillery School ATTN: APSF-CD-W, LT Monigal Fort Sill, OK 73503
1	Commander US Army Tank Automotive Research and Development Command ATTN: DRDTA-UL Warren, MI 48090	2	Commander Naval Surface Weapons Center ATTN: J. East Tech Lib Dahlgren, VA 22338
6	Project Manager Cannon Artillery Weapons System ATTN: DRCPM-CAWS, COL Phillip DRCPM-CAWS-AM, F. Menke H. Hassman DRCPM-CAWS-GP, B. Garcia DRCPM-CAWS-WP, H. Noble DRCPM-SA, J. Brooks Dover, NJ 07801	1	Commander Naval Weapons Center ATTN: Tech Lib China Lake, CA 93555
3	Project Manager M110E2 Weapons System ATTN: DRCPM-M110E2-TM, S. Smith R. Newlon B. Walters Rock Island, IL 61299	3	Commander Naval Ordnance Station ATTN: F.W. Robbins S.E. Mitchell Tech Lib Indian Head, MD 20640
		1	Director Lawrence Livermore National Laboratory ATTN: L355, A.C. Buckingham P.O. Box 808 Livermore, CA 94550

DISTRIBUTION LIST

<u>No. of Copies</u>	<u>Organization</u>	<u>No. of Copies</u>	<u>Organization</u>
1	Director Los Alamos Scientific Laboratory ATTN: D. Durak Los Alamos, NM 87545	1	Pennsylvania State University Department of Mechanical Engineering ATTN: K.K. Kuo University Park, PA 16801
1	Director Los Alamos Scientific Laboratory ATTN: Group T-7, B. Wendroff Mail Stop 233 Los Alamos, NM 87545	1	Princeton University Guggenheim Laboratories Department of Aerospace and Mechanical Science ATTN: L.H. Caveny P.O. Box 710 Princeton, NJ 08540
1	Calspan Corporation ATTN: E.B. Fisher P.O. Box 400 Buffalo, NY 14221	1	Rensselaer Polytechnic Institute Mathematical Sciences Department ATTN: D. Drew Troy, NY 12181
1	Paul Gough Associates, Inc. ATTN: P.S. Gough P.O. Box 1614 Portsmouth, NH 03801	1	University of Cincinnati ATTN: A. Hamed Cincinnati, OH 45221
3	Scientific Research Associates, Inc. ATTN: H. McDonald R.C. Buggeln H.F. Gibeling P.O. Box 498 Glastonbury, CT 06033	1	University of Cincinnati Department of Aerospace Engineering ATTN: W. Tabakoff Cincinnati, OH 45221
1	Massachusetts Institute of Technology Department of Materials Science and Engineering ATTN: J. Szekely 77 Massachusetts Avenue Cambridge, MA 02139	1	University of Delaware Department of Mathematical Science ATTN: M.Z. Nashed Newark, DE 19711
1	New York University Graduate Center of Applied Sciences ATTN: M. Summerfield 26136 Stuyvesant New York, NY 10003	1	University of Illinois College of Engineering Department of Aeronautical and Astronautical Engineering ATTN: H. Krier Urbana, IL 61801

DISTRIBUTION LIST

<u>No. of Copies</u>	<u>Organization</u>	<u>No. of Copies</u>	<u>Organization</u>
1	University of Illinois-Urbana Mechanics and Industrial Engineering ATTN: S.L. Soo Urbana, IL 61801		
1	University of Maryland Institute of Physical Sciences and Technology ATTN: S.I. Pai College Park, MD 20742		
1	University of Wisconsin-Madison Mathematics Research Center ATTN: J.R. Bowen 610 Walnut Street Madison, WI 53706		
1	Worcester Polytechnic Institute Department of Mathematics ATTN: P.W. Davis Worcester, MA 01609		

Aberdeen Proving Ground

Dir, USAMSA
ATTN: DRXSY-D
DRXSY-MP, H. Cohen

Cdr, USATECOM
ATTN: DRSTE-TO-F

Dir, USA MTD
ATTN: STEAP-MT-A, W. Rieden
C. Herud
H. Bechtol

Dir, USA CSL
ATTN: DRDAR-CLB-PA
Bldg. E 3516, APG-EA

USER EVALUATION OF REPORT

Please take a few minutes to answer the questions below; tear out this sheet, fold as indicated, staple or tape closed, and place in the mail. Your comments will provide us with information for improving future reports.

1. BRL Report Number _____
2. Does this report satisfy a need? (Comment on purpose, related project, or other area of interest for which report will be used.)

3. How, specifically, is the report being used? (Information source, design data or procedure, management procedure, source of ideas, etc.)

4. Has the information in this report led to any quantitative savings as far as man-hours/contract dollars saved, operating costs avoided, efficiencies achieved, etc.? If so, please elaborate.

5. General Comments (Indicate what you think should be changed to make this report and future reports of this type more responsive to your needs, more usable, improve readability, etc.)

6. If you would like to be contacted by the personnel who prepared this report to raise specific questions or discuss the topic, please fill in the following information.

Name: _____

Telephone Number: _____

Organization Address: _____

